

Origin and tectonic evolution of the metamorphic sole beneath the Brooks Range ophiolite, Alaska

R. A. Harris*

Department of Geology, West Virginia University, Morgantown, West Virginia 26506

ABSTRACT

Structural field relations, petrologic and geochemical studies, and radiometric age analysis of metamorphic rocks at the base of the Brooks Range ophiolite provide a record of the time, tectonic setting, and initial conditions of ophiolite emplacement during the Middle Jurassic western Brookian orogeny. The metamorphic sole of the Misheguk, Siniktanneyak, and Avan Hills ophiolite bodies is transitional with and geochemically similar to basalt, chert, limestone, and psammitic material mostly of the Copter Peak allochthon. Dynamothermal metamorphism of these rocks produced garnet-bearing amphibolite and quartz-mica schists that decrease in metamorphic grade and ductile strain intensity downward. These high-grade rocks are separated by thin, fault-bounded intervals from underlying greenschist facies and unmetamorphosed basalt and sedimentary rocks. The maximum total thickness of both parts of the metamorphic sole is <500 m.

Minimum temperature estimates, from garnet-biotite and garnet-amphibole geothermometric studies of rocks currently 5–50m below the ophiolite, range from 500 to 560°C at around 5 Kb. These conditions are similar to closing temperatures estimated for Ar retention in hornblende near the base of the ophiolite, which yields $^{40}\text{Ar}/^{39}\text{Ar}$ ages of 164–169 Ma. This age is concordant with, but slightly younger than the mean age of ophiolite crystallization. The limited time between crystallization and tectonic emplacement of the Brooks Range ophiolite, and compositional similarities between the metamorphic sole and continental margin material imply spacial and temporal proximity of the ophiolite with the Brookian orogen prior to emplacement.

Localization of strain at the base of the ophiolite during emplacement produced a ductile shear zone in the metamorphic sole that is characterized by mylonitic textures overprinted by postmetamorphic deformation. Microstructures document synkinematic crystal growth at high flow stress and strain rates. Kinematic indicators show mostly top-to-northwest sense of shear at the base of the ophiolite. Postmetamorphic deformation associated with the Brookian orogen shuffled various parts of the metamorphic sole and thrust it over shelf facies sedimentary material.

INTRODUCTION

Nappes of mafic and ultramafic igneous sequences commonly form the uppermost thrust sheets of imbricated continental

margin successions in many collisional mountain systems. These allochthonous igneous sequences are loosely termed “ophiolites” or “Alpine-type” ultramafics (Coleman, 1977). Other classification schemes such as “Tethyan- or Cordilleran-type” ophiolites (Moores, 1982) are also used to distinguish between ophiolites thrust over continental margins (Tethyan-type) and those that form terrane collages (Cordillerian-type). Although ophiolites

*Present address: Department of Geology, Brigham Young University, Provo, Utah 84602.

Harris, R. A., 1998, Origin and tectonic evolution of the metamorphic sole beneath the Brooks Range ophiolite, Alaska, in Oldow, J. S., and Avé Lallemant, H. G., eds., Architecture of the Central Brooks Range Fold and Thrust Belt, Arctic Alaska: Boulder, Colorado, Geological Society of America Special Paper 324.

represent a diverse assortment of tectonomagmatic settings (Coleman, 1984), most Tethyan-type ophiolites are chemically similar to oceanic island arc-complexes (Pearce et al., 1984). The similar structural position and tectonic associations of these ophiolites in different continental fold-thrust belts suggest common mechanisms for emplacement.

A very important feature of many Tethyan-type ophiolite nappes are the thin sheets of metamorphic rock at their structural bases (i.e., Williams and Smyth, 1973; Searle and Malpas, 1980; Ghent and Stout, 1981; Moores, 1982; Jamieson, 1986). These metamorphic rocks (herein referred to as metamorphic soles) form part of the basal shear zone of ophiolite nappes and are characterized by an inverted sequence of amphibolite- and greenschist-facies metabasalt (mostly E- and T-type mid-oceanic ridge basalt [MORB]), metachert, and marble. The shear zone commonly juxtaposes the metamorphic sole with structurally underlying distal facies continental margin deposits. Locally these deposits are structurally omitted placing the metamorphic sole directly on proximal facies shelf units. This structural contact represents an early collisional plate boundary that was uplifted by subsequent accretion of lower plate material in the collision zone.

Rocks incorporated into the metamorphic sole represent some of the first material to underthrust the "hot" ophiolite after detachment from its roots and before cooling. Determining the protolith, structural evolution, and timing and conditions of metamorphism of the metamorphic sole may constrain the tectonic setting, temperature, transport direction, and even the minimum age of initial ophiolite emplacement. These data are critical for resolving various models for the tectonic affinity of ophiolites and determining the temporal and spatial relations between ophiolites and the orogenic belts where they reside.

The Brooks Range ophiolite has a metamorphic sole of garnet-bearing amphibolite and quartz-mica schist, greenschists, and metabasalt, chert, marble, and psammitic material. Since the first general field descriptions of the Brooks Range ophiolite were published by Snelson and TAILLEUR (1968) and MARTIN (1970), interpretations of its ophiolitic associations and tectonic significance have relied on sparse data from reconnaissance-style studies (i.e., PATTON et al., 1977; ROEDER and MULL, 1978). The purpose of this paper is to present data collected along several structural transects through the metamorphic sole of the Brooks Range ophiolite, which is exposed mostly at the base of the Mishéguk Mountain and Avan Hills ophiolite bodies (Fig. 1).

REGIONAL OVERVIEW

The Brooks Range allochthon belt (Mayfield et al., 1983) comprises the western 200–300 km of the Brooks Range fold-thrust mountain system of Arctic Alaska (Fig. 1). The western Brooks Range exposes the highest structural levels that are eroded from the central and eastern part of the orogen. The stratigraphic record of the western Brooks Range represents a long interval of passive continental margin development. These conditions persisted from early Paleozoic to the Middle Jurassic onset of orogenesis. The passive margin was shortened by collision with arc

terraces of the Yukon-Koyukuk province (Roeder and Mull, 1978; Box, 1985; Harris, R. A., et al., 1987), which is presently south of the Brooks Range (Fig. 1). The initial phases of this collision involved detachment and tectonic emplacement of large ophiolitic thrust sheets, which are partially preserved in the western Brooks Range. The final pulses of the orogen are associated with basement involved thrusting and rapid hinterland unroofing (Gottschalk and Oldow, 1988; Till et al., 1988). An extensive blueschist belt is exposed in the hinterland (Patton et al., 1977).

The shear zone at the structural base of the Brooks Range ophiolite served as the initial plate boundary between underthrust continental material and impinging arc terranes of the upper plate. Metamorphic rocks in this shear zone provide an important record of these events. Relocation of the plate boundary during and after accretion determines to a large extent how well the earlier tectonic features associated with ophiolite emplacement are preserved. In the western Brooks Range, as in Oman (Searle and Malpas, 1980; Harris, 1992), postcollision deformation was minimal and subjected the fold-thrust mountains to only minor subsequent structural and thermal overprints. This differs from most other parts of the North American Cordillera that were intensely modified by Laramide and subsequent phases of deformation (e.g., Moores, 1970).

The structural relations preserved in the western Brooks Range indicate hundreds of kilometers of passive margin contraction associated with emplacement of extensive ophiolite sequences (Martin, 1970; TAILLEUR, 1970; Mull, 1982; Mayfield et al., 1983). Arctic Alaska is now bounded by two principal geologic features: a passive continental margin to the north and a collisional margin known as the Kobuk suture to the south. The Kobuk suture separates Arctic Alaska from arc terranes of the Yukon-Koyukuk province (Fig. 1) in the hinterland of the Brooks Range. The metamorphic sole at the base of the Brooks Range ophiolite is also considered part of this suture zone.

Brooks Range ophiolite

The Brooks Range ophiolite consists of mafic and ultramafic thrust sheets that form five different klippen-like massifs of con-sanguineous composition, internal organization, structure, and age (Harris, 1995). The massifs are known from west to east as Iyokrok, Asik, Avan Hills, Misheguk, and Siniktanneyak (Fig. 1). The ophiolite bodies most likely represent fragmented and eroded remnants of what was initially an extensive roof thrust perhaps as large as 350 km in strike length, 50 km in width, and as much as 3–4 km thick.

The composition of the Brooks Range ophiolite consists of the following igneous sequence in ascending order: (1) tectonized peridotites, (2) ultramafic cumulates, (3) layered gabbro, (4) massive gabbro and high-level intrusives, (5) out-of-sequence intrusives, and (6) rare sheeted dikes, lavas, and sediments (Harris, 1995). The various units are most commonly transitional except for local intrusive relations. Chemically, the Brooks Range ophiolite is typical of ophiolites that are transitional between MORB- and arc-types (Harris, 1992, 1995). Transitional-type ophiolites are considered by Pearce et al. (1984) to represent tholeiitic magmas derived from

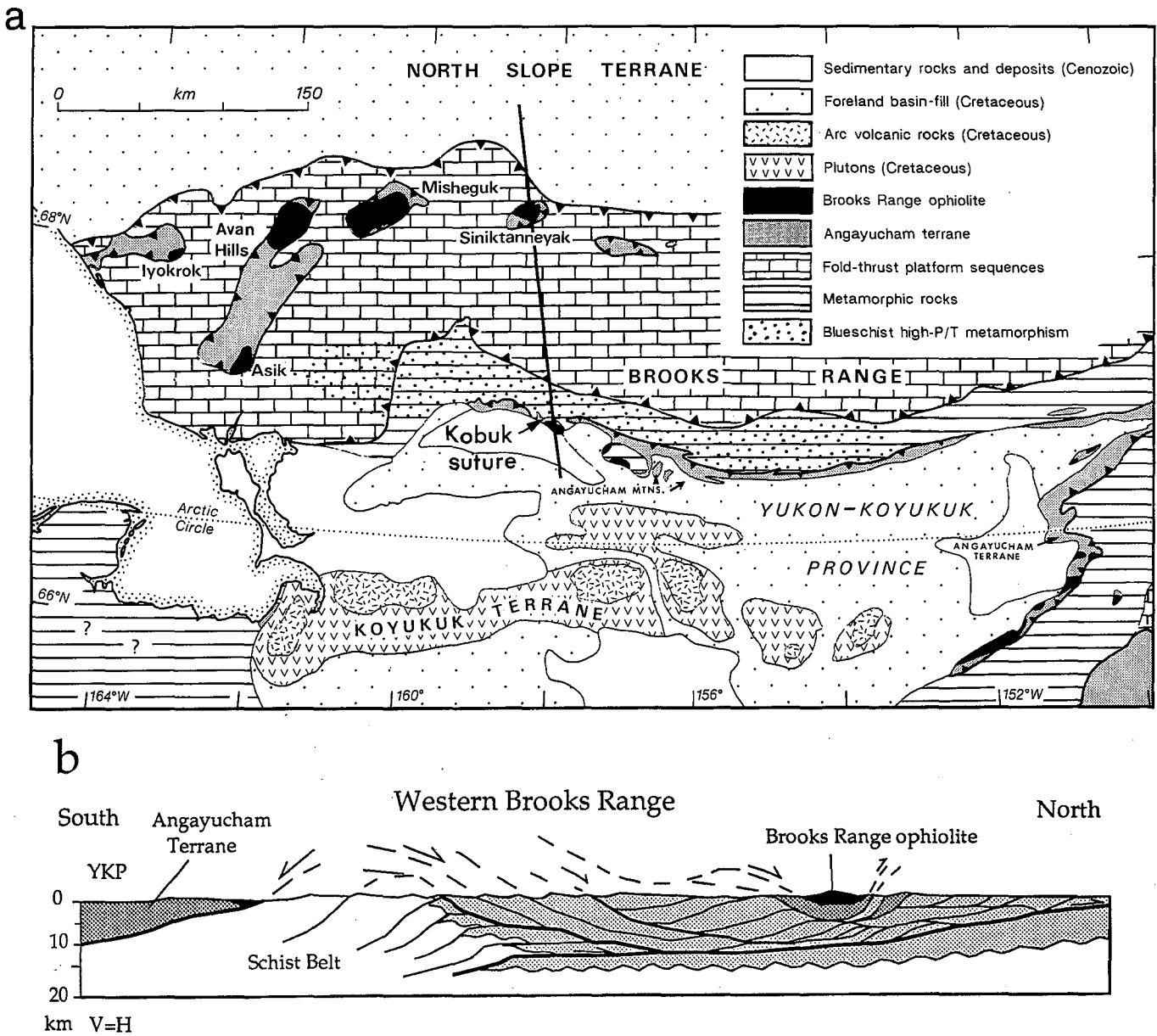


Figure 1. Geology of the western Brooks Range and northern Yukon-Koyukuk province (modified from Patton, 1973). a, Simplified geologic map. b, Schematic cross section showing the Brooks Range ophiolite nappe (black), Copter Peak allochthon/Angayucham terrane (dark gray), pre-Mississippian basement (white), and sedimentary cover sequences (light gray). The roots of the ophiolite nappe are interpreted as the mafic and ultramafic plutonic rocks that structurally overlie basalts and chert of the Angayucham Mountains region. YKP = Yukon-Koyukuk province.

partial melts of a moderately depleted mantle. Modern examples of thin oceanic crust with transitional-type geochemistry are documented from small ocean basins in the western Pacific, Scotia, and Andaman Seas. Most of these basins formed by processes of intra-arc spreading (Moores et al., 1984; Pearce et al., 1984).

Angayucham terrane

Along the Kobuk suture zone of the southern Brooks Range the Angayucham Mountains (Fig. 1) expose a narrow, curvilinear

belt of Devonian to Early Jurassic pillow basalt, diabase, basaltic tuff, and radiolarian chert (Patton et al., 1977; Pallister et al., 1989). Structurally overlying the basalt-chert terrane are fragments of mafic and ultramafic thrust sheets of the Brooks Range ophiolite (Patton and Box, 1989; Harris, 1992). The gross similarity of the two separate allochthonous masses initially led to incorrect correlations that lump the Brooks Range ophiolite with the Angayucham terrane (Jones et al., 1981; Box, 1985; Moore and Grantz, 1987; Plafker, 1988).

Copter Peak allochthon

In the western Brooks Range fold-thrust zone, Angayucham-like volcanic and sedimentary rocks are known as the Copter Peak allochthon (Elliessieck et al., 1982). Thrust sheets of the Copter Peak allochthon commonly form the uppermost structural elements of the western Brooks Range fold-thrust belt, except where they are structurally overlain by Brooks Range ophiolite massifs. The Copter Peak allochthon has remnants of thick mafic igneous crust that consist of amygdaloidal and vesicular pillow and massive basalt and, to a lesser extent, felsic lavas and diabase. Chert, tuff, carbonate, and some clastic detritus are tectonically interleaved with the igneous rocks. Chert layers yield Pennsylvanian–Upper Triassic radiolaria (Nelson and Nelson, 1982; Elliessieck et al., 1982) and may be correlative with distal rise deposits of the Arctic Alaskan passive continental margin (Etivluk Group). Most of the carbonate is similar in facies and fauna to Devonian sections of para-autochthonous shallow-water limestones (Baird Group limestone, see Dumoulin and Harris, 1987). The structural relations between limestone and volcanic rocks of the Copter Peak allochthon are ambiguous. Mayfield et al. (1983) considered the carbonate as part of continental margin material that was tectonically slivered with volcanic rocks. Nelson and Nelson (1982) claim stratigraphic continuity from pillow lavas into carbonate with Devonian fauna and rounded pebbles of basalt.

Lithologic, biostratigraphic, and structural similarities justify including the Copter Peak allochthon as part of the Angayucham terrane. The basalt, chert, and other rocks associated with this terrane were accreted to the base of the Brooks Range ophiolite at the onset of the Brookian orogeny.

Geochemistry of the Angayucham/Copter Peak igneous rocks

Geochemical studies of Copter Peak allochthon igneous rocks yield similar results to basalts of the Angayucham terrane in the Kobuk suture (Harris, 1987; Moore, 1987; Wirth et al., 1987). Both complexes consist of tholeiites and some compositions transitional to alkali-basalt. Trace-element discriminant analysis of the lavas yields N- and T-type MORB trends with mostly “within-plate basalt” associations. These chemical affinities are found in many intraplate tectonic settings. Geochemical data from volcanic material in the Kobuk suture zone is interpreted by Barker et al. (1988) and Pallister et al. (1989) as ocean-plateau and ocean-island basalts. These rocks are also similar to basalts from distal continental margins. Examples of thick (10 km) deposits of N- and T-type MORB lavas exist along the Norwegian-Rockall and conjugate east Greenland banks; outer Scott, Wallaby, and Naturaliste plateaus of Western Australia; and the southeast Weddell Sea of Antarctica (Mutter et al., 1988). A distal continental margin origin for the basalt-chert terrane is also supported by stratigraphic relations between the sedimentary sequence interbedded with lavas and continental margin sequences of Arctic Alaska (Dumoulin and Harris, 1987; Alexander, 1990).

Although igneous geochemistry is limited in distinguishing between possible tectonic settings of transitional-type ophiolites,

it is useful for discriminations between igneous rocks of significantly different lineage. Geochemical differences between the igneous rocks from the Brooks Range ophiolite and the Angayucham terrane preclude any genetic relation between them (Harris, 1992, 1995). The melts that formed the Brooks Range ophiolite had a moderately depleted source compared with the normal and enriched sources for Angayucham terrane lavas. Although a range of possibilities exists for the tectonic setting of both igneous complexes, there is little potential for overlap.

The Angayucham igneous complex documents a long interval of intraplate-type magmatism associated, at least in part, with the development of the Arctic Alaskan passive continental margin. The formation of the Brooks Range ophiolite immediately proceeds the contraction of this margin and juxtaposition of the two different igneous terranes. The timing and conditions of accretion of the two terranes are constrained to some extent by the thin metamorphic complex that locally occurs between them.

SUBOPHIOLITE METAMORPHIC COMPLEX

Glacial incisions through klippen of the Brooks Range ophiolite expose its structural base and metamorphic sole at several locations over a distance of 130 km. Reconnaissance descriptions of these metamorphic rocks are available for the Avan Hills (Zimmerman and Frank, 1982; Harding et al., 1985; Wirth et al., 1986), Misheguk (Harris, 1987), and Iyokrok (Boak et al., 1987) ophiolite bodies. The most extensive and complete occurrence is at Misheguk, which together with the Avan Hills metamorphic sole are the focus of this investigation.

At Misheguk the metamorphic sole forms a series of north-east-southwest-trending dark-colored hills along the northwest flank of the ophiolite body (Fig. 2). The metamorphic sole is characterized by intercalations of black amphibolite, maroon and black metasedimentary schists, dark green metavolcanic rocks, and cream-colored metachert. The rocks are generally fine grained with a strong, commonly mylonitic, layer-parallel foliation.

Field relations

Table 1 provides a description of mineral parageneses from twelve traverses through the metamorphic sole at Misheguk shown in Figure 2. Mineral parageneses are listed relative to distances from the structural base of the Brooks Range ophiolite, which is signified by “gz” (gouge zone) on Figure 2.

Traverses 1–4. Northwest of Misheguk Mountain metamorphic sole rocks underlie tectonized peridotite and dunite (Fig. 3a). The complex consists of 0–40 m of garnet amphibolite, which overlies a low-grade (greenschist facies) assemblage with mafic volcanic and pelagic sedimentary protoliths. The low-grade rocks are less than 200 m thick and decrease in grade downward toward unmetamorphosed distal facies continental margin deposits and melange. Faults structurally thin and eventually eliminate the metamorphic sole along strike, sometimes juxtaposing the ophiolite complex with Devonian and younger Baird Group carbonate, Etivluk Group pelagic material, and Cretaceous Okpikruak Formation.

Traverses 5–9. On the northeast flank of Misheguk Mountain metamorphic sole rocks underlie cumulate ultramafic rocks and layered gabbro (Fig. 3b). The mantle sections of the Brooks Range ophiolite are structurally omitted. Immediately below the cumulate sequence is a thick (as much as 50 m) fault gouge zone composed of phacoidal blocks (as much as 5 m in diameter) of mylonite, serpentinite, tectonized peridotite, gabbro, and rodingite floating in a dominantly serpentinite matrix. Veins of calcite and prehnite intrude the gouge zone. The fault gouge is underlain by a thin (0–30 m) band of garnet-bearing amphibolite and quartz-mica schist. The schists grade in broken succession downward into greenschists followed by altered melange, volcanics, pelagics, and carbonates of the Copter Peak allochthon. The metamorphic complex strikes east-northeast toward the north flank of peak 1217, maintaining a structural thickness of about 1.5 km.

Traverses 10–12. Dark green amphibolitic metabasalt with locally preserved igneous textures is exposed for about 1 km along a continuous ridge on the north flank of peak 1217 (Fig. 2 and 3c). The emplacement fault and inverted metamorphic complex dip steeply and are locally overturned by as much as 30° (dip 60° north). Faulted slivers of porphyroclastic harzburgite and lherzolite, and 2.5 km of massive dunite, which originally overlay the metamorphic complex, now underlie it along an overturned thrust.

The overturned metamorphic complex consists of an imbricate sequence of fault slices that range in thickness from 50 to 120 m (Fig. 3c). Metamorphic grade and deformation intensity decrease upward away from the Brooks Range ophiolite in each overturned slice and throughout the imbricate stack toward altered mafic lavas of the Copter Peak allochthon. Copter Peak volcanic rocks are juxtaposed with greenschists of the metamorphic complex along a north-dipping fault, which is also overturned. Scaly clay melange with blocks of Copter Peak volcanic rocks, Etivluk Group chert, and some metamorphic clasts surround the overturned sequences (Fig. 3c).

Traverse of the Avan Hills. The Avan River drains a glacial valley cut through the Avan Hills ophiolite body into the structurally underlying Copter Peak allochthon (Fig. 3d). Subophiolite metamorphic rocks, serpentine, and tectonized harzburgites are found at several locations along the flat-lying structural base of the ophiolite. Thin layers (few decimeters) of lower-greenschist-facies metabasalt, garnet amphibolites, and granitic mylonites were found during this study. The granitic material intrudes the base of the ophiolite nappe only for a distance of a few meters and is subsequently deformed. Mylonitic fabrics in these rocks are most intense at the structural base of the nappe.

Structure

The metamorphic sole documents a complex multiphase history of ductile and brittle deformation associated with emplacement and fragmentation of the Brooks Range ophiolite. The largest remnants of the metamorphic sole are found on the north flank of Misheguk Mountain, where most of the measurements for this study were obtained. In this region metamorphic rocks

form a thrust and folded stack as much as 1,200 m thick that trends east-northeast to west-southwest. High-angle oblique slip faults offset the structural stack of metamorphic rocks locally (Fig. 2). Basalt, chert, and limestone of the Copter Peak allochthon form thrust sheets and broken formation within the stack. Structures were also analyzed from poorly exposed outcrops of the metamorphic sole at Avan Hills and Siniktanneyak.

The internal structure of the metamorphic sole is dominated by a layer-parallel mylonitic schistosity (S1), which is associated with D1 and was subsequently folded and fractured by post-peak metamorphism deformation, D2. Poles to S1 foliation plot along a north-northwest to south-southeast girdle with a pole near to the mean of F2 axes (Fig. 4a). Layer parallelism is demonstrated by the overlap between the poles of foliations and folded chert layers near the base of the metamorphic sole (Fig. 4b).

Three phases of folding are recognized in the metamorphic sole. The first phase (F1) is found in helicitic garnet inclusions (Fig. 5), rotated porphyroclasts, and northwest-vergent isoclinal microfolds associated with S1. F2 folds are more obvious in the field because they modify the entire thrust stack. These folds have southeast-dipping axial planes (Fig. 4c), which indicate vergence to the northwest. Locally these folds overturn sections of the ophiolite and the metamorphic sole (Fig. 3c). F3 folds are poorly developed, have a low amplitude, long wavelength, and plunge steeply to the southeast (Fig. 4c).

Two major sets of faults are found (Fig. 4d). North-south-striking faults are commonly associated with S1 foliations and are interpreted as forming during D1. East-west-striking faults include those forming the base of the Brooks Range ophiolite at Misheguk, Avan Hills, and Siniktanneyak. Major discontinuities in metamorphic grade occur across these faults, which are associated with top-to-the-northwest, F2 folds. Grooves on fault surfaces associated with the basal thrust of the Brooks Range ophiolite trend north-south. A variety of groove orientations were found on other faults, which produce an ambiguous kinematic pattern. Grooved fault surfaces indicate that latest motion along many faults was near horizontal. Crosscutting and abutting mode 1 fractures mostly trend north-south, which may indicate the orientation of stresses after faulting.

Microstructures show various effects of inhomogeneous rotational shear overprinted locally by static crystal growth (Fig. 5). Most early, foliation-forming mineral grains show strong dimensional preferred alignment, streaky mylonitic foliation, and lenticular porphyroclasts of strained plagioclase, amphibole, and snowball and helicitic garnet that are enclosed by sheety and fibrous silicates with rotational asymmetry.

Shear-sense indicators such as asymmetric augen structures and pressure shadows, composite or s-c planar fabrics, mica “fish,” asymmetric microfolds, shape-preferred orientations, mineral stretching lineations, and displaced broken grains were inspected in thin sections oriented parallel to D1 lineations. These structures show a top-to-the-northwest displacement during the earliest recorded and most penetrative phase of deformation.

Deformation mechanisms

Dynamic recrystallization of quartz formed subgrains and neoblasts by mechanisms of grain boundary migration and subgrain rotation distortions. In amphibolite-grade sections of the metamorphic sole, quartz shows evidence of near-complete recovery. Many layers have equant, strain-free subgrains with 120 triple junctions. Other layers have more irregular, bulging grain boundaries, and preserve deformation bands. Polycrystalline quartz ribbons are common (Fig. 5c and d). Quartz grains in lower amphibolite and greenschist facies parts of the metamorphic sole are larger, with more common deformation bands, and serrated grain boundaries.

The softening effect of dynamic recrystallization caused localization of strain that is documented in the metamorphic sole by changes in quartz subgrain diameter. Under steady-state conditions grain size reduction is a function of flow stress and is essentially temperature independent (Twiss, 1986). Quartz subgrain diameters were measured in oriented thin sections from throughout the metamorphic sole (Table 1). Most samples yield a unimodal distribution of grain size where 60–70% of the grains vary by only 3 μm . Quartz subgrain sizes range from 4.13 to 8.14 μm within 20 m of the ophiolite, and from 6.00 to 10.70 μm between 20 and 70 m from the ophiolite (Table 1). Traverse 11 shows the most systematic trend of reduced grain size toward the basal contact of the ophiolite.

Applying the results of laboratory piezometric studies (Mercier et al., 1977; Schmid, 1982; Twiss, 1986) to the size of quartz subgrains in the metamorphic sole predicts flow stresses of 150–200 MPa within 20 m of the ophiolite, and 80–160 MPa 20–70 m below the contact. The deformation mechanism map of Rutter (1976) predicts that at temperatures of 500–600°C and flow stresses greater than 100 MPa that quartz will deform by dislocation glide at rapid strain rates of 10^{-10} s^{-1} to 10^{-9} s^{-1} .

Crystal plastic deformation of other minerals indicate similar dynamothermal metamorphic conditions to those of quartz. Calcite grains between 40–100m below the ophiolite range from 0.5–3 μm in diameter, which is consistent with yield stresses 40–70 MPa at room temperature (Olsson, 1974). K feldspar is slightly recrystallized within 20 m of the base of the ophiolite, which initiates in laboratory tests at temperatures of more than 500°C (Kronenberg and Shelton, 1980).

Crystal plastic deformation was followed locally by thermal annealing producing blastomylonitic and hartschier textures in some amphibolitic sections of the metamorphic sole. Cross-micas, helicitic and idioblastic garnet and amphibole, polygonization, and chlorite and epidote pseudomorphism locally crosscut foliations. Some clasts have much coarser, randomly oriented grains than the matrix fabric, and preserve various relict phases of the metamorphic history. The transition from D1 layer-parallel flattening to D2 folds accompanies the annealing and subsequent passage of the rocks through the brittle-ductile transition.

Brittle disruption of ductile fabrics by faults, fractures, cataclasis, and veining indicate low temperatures or high strain rates

during the final phases of ophiolite emplacement. Low-grade mineral-filled veins are associated with metamorphic retrogression and high fluid pressures. Early crosscutting and some layer-parallel fractures are sealed by secondary mineral deposits (albite, prehnite, calcite, chlorite, and sometimes epidote and pumpellyite) possibly associated with serpentinization of the overlying Brooks Range ophiolite.

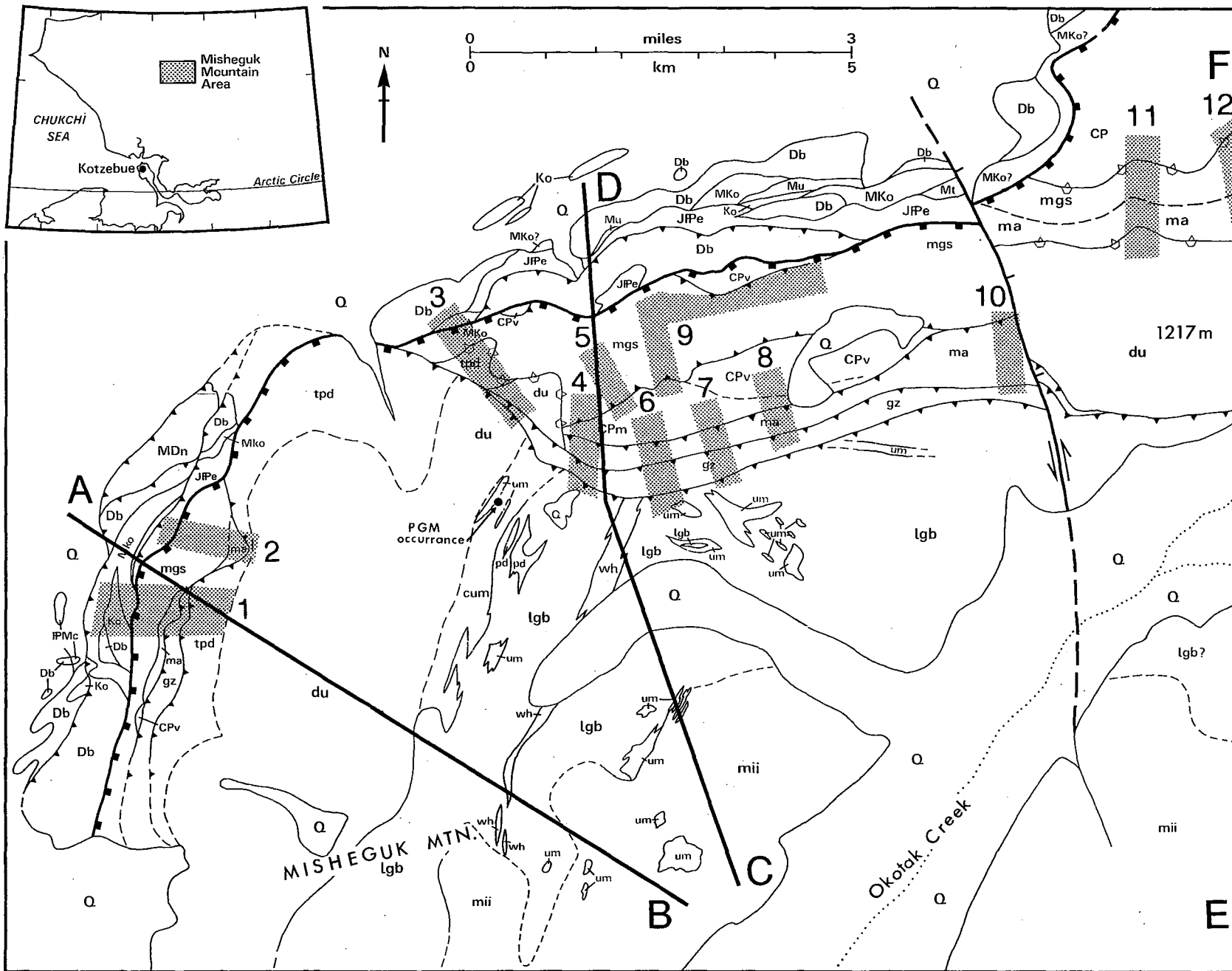
Petrology and mineral paragenesis

Lithologic descriptions of samples from traverses made through the metamorphic sole and into immediate underlying rocks are provided in Table 1. Lateral discontinuities and post-metamorphic faulting make it difficult to correlate individual lithologic units between traverses. However, where thick sections of the metamorphic sole are exposed, a similar lithologic succession is found. This succession consists, in descending order, of: (1) a zone of cataclasis and partial melt intrusion at the structural base of the ophiolite, (2) amphibolite and quartz-mica schists, (3) greenschist facies metavolcanic and metasedimentary rocks, and (4) volcanic and sedimentary rocks of the Copter Peak allochthon and underthrust continental margin sequences (described above). Metamorphic rocks form two distinct units that are referred to as the upper or amphibolite unit and lower or greenschist units of the metamorphic sole.

The initial thickness and metamorphic gradient of the succession are difficult to estimate due to postmetamorphic deformation. North of Misheguk Mountain the metamorphic sole is commonly structurally thickened, whereas west of Misheguk Mountain, and at Avan Hills and Siniktanneyak, most of the



Figure 2. Geologic map of the western Misheguk Mountain ophiolite body, its metamorphic sole, and underlying thrust sheets. Positions of traverses through the metamorphic sole are shown in stippled areas and numbered for reference to text. Lines of section in figure 3 are shown. Abbreviations are for figures 2 and 3: *Ophiolite units* (in descending stratigraphic order): mii - mafic and intermediate (high level) intrusives; um - ultramafic out-of-sequence intrusives; lgb - layered gabbro; PGM - Platinum group metal; tz - transition zone; wh - wehrlite; cum - cumulate ultramafics; du - dunite; pd - peridotite; tpd - tectonized peridotite; serp - serpentinite; gz - gouge zone. *Metamorphic Sole units (MS)*: ma - amphibolite-facies rocks; mgs - greenschist-facies rocks. *Copter Peak complex (CP)*: CPv - volcanics; CPmm - metasediments and metavolcanics; CPc - chert. *Pre-rift continental margin sequences*: Db - Devonian Baird Group carbonates; MDn - Mississippian and Devonian Noatak sandstone and conglomerates; Mko - Mississippian Kogruk Formation deep-water limestones and chert; Mls - Mississippian limestone; Mt - Mississippian Tupik Formation limestone and chert; Mu - Mississippian Utukok formation limestone, sandstone, and shale. *Post-rift passive continental margin sequence*: PMc - Pennsylvanian and Mississippian radiolarian chert; JPe - Jurassic to Pennsylvanian Etivluk Group chert and shale; JPM - mafic dikes and sills. *Syn- and post-orogenic sedimentary rocks*: KJo - Cretaceous (Ko) and Jurassic Okpikruak Formation (melange and broken formation with interbedded conglomerate, sandstone, and remobilized shale); Q - Quaternary alluvium. *Structural symbols*: Faults - shown in heavy lines. Faults with filled square teeth have omitted lithotectonic units. Faults with open, nested teeth are overturned thrusts.



Origin and tectonic evolution of metamorphic sole beneath the Brooks Range ophiolite

TABLE 1. MINERAL PARAGENESSES AND QUARTZ SUBGRAIN SIZE

Distance (m)	Mineral Parageneses*	Qtz SGS	N	Distance (m)	Mineral Parageneses*	Qtz SGS	N
Traverse 1				150-200 dn	Chl+ab+qtz		
30 up	Dunite			200 dn	Spilitic basalt		
30 up	Lherzolite			200 dn	Radiolarian chert		
30 up	Lherzolite + harzburgite			Traverse 8			
20 up	Harzburgite			0-10 up	Websterite + lherzolite		
3 up	Grt+pl+chl+ep+op			10-20 dn	Am+chl+pl(An30)+ep?		
0	Harzburgite			40-50 dn	Chl+act+ab+ep+qtz	8.24	425
1 dn	Qtz+chl+wm+grt	4.55	200	Fault			
1 dn	Qtz+fld+am			50-60 dn	Volcaniclastic w/ chert frag		
1 dn	Grt+am+cal+qtz+chl+pl+spn	4.72	200	60-100 dn	Spilitic basalt		
1 dn	Am+ep			Traverse 9†			
1 dn	Grt+bt+qtz+chl+am+ab+ep+/-wm	4.84	225	20-50**	Qtz+bt+grt+pl(An29-36)+chl+py	6.00	200
10-20 dn	Act+ab+chl+ep (relict px+ab)			20-50	Act+chl+ab+ep+cal+op	8.10	365
20-30 dn	Cherty argillite			800	Meta cpx basalt		
30 dn	Fossiliferous marble			800	Act+pl+chl+qtz+ep+op		
Traverse 2				800	Qtz-chl schist		
10 up	Harzburgite			1200	Am+pl+ep+chl+op		
3 dn	Qtz+chl+act			1400	Am+pl+ep+chl+op		
20 dn	Ab-or+act+chl+ep+/-spn			1400	Am+pl+ep+chl+op		
40 dn	Marble			1600	(Rd+bk) knarly chert		
40 dn	Purple and green cherty argillite			1600	Fossiliferous limestone		
Traverse 3				800-1200	Bt+cal+qtz+op		
30-40 up	Lherzolite			800-1200	(Grn)cherty argillite		
1 up	Lherzolite			800-1200	(Bk+rd)chert+argillite		
1 up	Srp+ol+chr			800-1200	Cal+chl+qtz+ep+grt		
10 dn	Relict ol?+cpx+pl+chl+ep+am			800-1200	Am+ab+ep+chl		
40 dn	Relict ol+cpx+pl/ab+chl+ep			800-1200	Interlayered chert + mafic rock		
Traverse 4				Traverse 10			
50 up	Srp			10 up	Srp harzburgite		
40 up	Harzburgite			10 dn	Am+qtz+ep		
40-30 up	Olivine gabbro			10-20 dn	Am+pl+qtz		
10 dn	Am+pl(An40)+spn+chl+ep+cal+hrn +/-wm+ap			50-60 dn	Chl+act+ep+qtz		
10 dn	Qtz+chl+ep+grt+/-wm	5.23	125	Traverse 11‡			
10 dn	Wm+qtz+op+ep+grt	8.14	50	5-10 dn	Srp harzburgite		
10-15 dn	Basalt			Fault gorge	Am+ep+chl+qtz+cal	3.80	90
15 dn	Qtz+chl+wm+op+ep	6.00	44	Block	Meta chert	5.32	330
Traverse 5†				Block	Pl+am+/-ep+/-qtz	5.90	81
30-50	Grt+qtz+bt/chl+ab+ep	4.13	164	10 dn	Qtz+am+chl+ep	6.92	25
200-300	(Rd+bk) qtz-mica schist			20 dn	Am+pl+qtz	7.08	36
300-350	Act+chl schist			27 dn	Ep+qtz+am+chl	8.50	120
350-400	Act+chl+ep+fld			32 dn	Am+ep+qtz+cal	8.40	25
500-600	(Rd+bk) qtz-mica schist	5.55	38	40 dn	Grt+qtz+wm+py+chl	9.50	249
700-800	Act+chl schist			65 dn	Am+ep+qtz		
1100-1200	Chl+qtz schist			70 dn	Am+ep+qtz (relict grains)	10.70	184
Traverse 6				90 dn	Am+pl+ep+chl		
20-30 up	Gabbro			90-100 dn	Qtz+am+chl+ep		
20 up	Gabbro+clinopyroxenite layers			105-125 dn	Meta-chert+meta-marls		
0	Altered gabbro+wehrlite cataclasis			135 dn	Meta-basalt		
0	Opx+srp			147 dn	Meta-chert		
10-20 dn	Hrn+opx+ep+ab			165 dn	Meta-basalt		
30-50 dn	Grt+hrn+wm+pl(An23)+ep+qtz	5.20	100	250 dn	Spilitic basalt + ls blocks		
150-200	Meta pillow basalt			Traverse 12			
200-250	Meta basalt			0-5 dn	Serpentinite		
Traverse 7				0-5 dn	Am+ep+qtz		
20 up	Gabbronorite			15 dn	Am+pl (meta-basalt)		
0	Dunite (+cpx+sp)			17 dn	Act+chl+pl		
0	Cpx+pl (Gabbro)			*Abbreviations after Kretz, 1983: ab-albite; act-actinolite; am-amphibole; ap-apatite; bt-biotite; cal-calcite; chl-chlorite; chr-chromite; cpx-clinopyroxene; ep-epidote; fld-feldspar; grt-garnet; hrn-hornblende; ol-olivine; op-opaque; opx-orthopyroxene; or-orthoclast; pl-plagioclase; px-pyroxene; py-pyrite; qtz-quartz; sp-spinel; spn-sphene; srp-serpentine; wm-white mica. SGS-subgrain size; N-number of grains counted; rd-red; bk-black; grn-green; up-above contact; dn-below contact; ls-limestone.			
0	Tectonized harzburgite			†Horizontal distance; §Sample 132b; **Sample 150; †Overturned.			
3	Cataclastite						
4-5 dn§	Qtz+ab+grt+wm+chl schist	4.70	200				
	hrn+grt+pl (An29-34)+opx+chl						
20 dn	Marble						
100-150 dn	Cpx+am+srp						

metamorphic sole is structurally omitted. The most complete section, representing what may be the original thickness of the metamorphic sole, is traverse 11 where a systematic reduction of grain size and increase in metamorphic grade is found toward the structural base of the ophiolite. At this location the base of the ophiolite is separated from the Copter Peak allochthon by 250 m of metamorphic rock.

1. Structural base of the Brooks Range ophiolite. The structural base of the Brooks Range ophiolite, immediately above the metamorphic sole, is characterized by foliated and fractured serpentinite with phacoidal blocks of porphyroclastic gabbro and peridotite that are encased in an orange, serpentine-rich fault-gouge. Where relict grains are preserved, they are recrystallized, undulose, bent, and fractured from the combined effects of crystal plastic and cataclastic flow-type deformational mechanisms. Intense veining and rodingization in this zone indicates the presence of high fluid pressures and temperatures.

At Siniktanneyak and Avan Hills minor granitic intrusions are found at the base of the Brooks Range ophiolite mantle sequence. Nelson and Nelson (1982) report small (1–5 m width), two-mica alaskite dikes (S-type granites) that intrude mylonitic dunite and peridotite immediately above the structural base of the Brooks Range ophiolite at Siniktanneyak. Further study of these dikes as part of this investigation found granodiorite, quartz-diorite, and tonalite compositions. Glassy quartz and albite(?) veins are also abundant. Most of the dikes are near-vertical, wedge-shaped prongs that narrow upward from the base of the ophiolite and pinch out only a few decimeters into the mantle sequence hanging wall. Some dikes have mylonitic textures, indicating that intrusion coincided with various stages of tectonic emplacement.

The concentration of granitic dikes along the structural base of the Brooks Range ophiolite mantle sequence, and the geometry and composition of the dikes, show that some partial melting was associated with thrusting of the hot ophiolite over felsic foot-wall rocks, as suggested in other settings by Clemens and Wall (1981). Harding et al. (1985) interpreted granitic dikes at the base of the Avan Hills peridotite as segregations of anatectic granitic melt. However, it is also possible that the dikes and particularly the veins are a product of solid-state diffusional processes related to solution mass transfer during metamorphism.

2. Amphibolite facies schists. Garnet-bearing amphibolite-grade schists and mylonites are widely distributed immediately below the structural base of mantle peridotites of the Brooks Range ophiolite. Locally these rocks are "welded" to the structural base of the ophiolite and occur as part of the hanging wall above fault-gouge zones. Compositional bands in the schists and mylonites are common and consist of alternating bands of mafic and felsic-rich material. The most common rock types are garnet-bearing amphibolites and quartz-mica schists. A discontinuous zone of epidote-amphibolite occurs in traverse 9 (Table 1).

The most common mineral parageneses in amphibolite grade schists are hornblende-plagioclase \pm garnet \pm epidote \pm quartz \pm chlorite \pm sphene \pm orthoclase \pm ilmenite. Accessory minerals include zircon, tourmaline, apatite, and iron oxides. The

relative proportions of hornblende to plagioclase, low abundance of quartz, relict igneous textures, and bulk chemistry suggest that the amphibolites have basaltic and gabbroic protoliths. At Avan Hills, Zimmerman and Frank (1982) reported the assemblage amphibole-plagioclase-quartz-orthopyroxene \pm garnet. However, orthopyroxene has not been found in any samples collected from the base of the Avan Hills body during this investigation. Along Kisimilot Creek, at the structural base of Iyokrok, Boak et al. (1987) report metabasite with hornblende-plagioclase \pm sphene \pm ilmenite mineral assemblages. The metabasites are associated with more dominant para-amphibolites with layered mineral assemblages of hornblende-plagioclase-quartz \pm biotite \pm garnet \pm ilmenite \pm sphene. Distinctions of para-amphibolite are based on the occurrence in some nonmylonitized layers of rounded plagioclase porphyroclasts interpreted as relict clastic feldspars.

Banded quartz-mica schists are commonly interlayered with amphibole-schists. At Misheguk, quartz-mica schists are fine grained and consist of folded, alternating layers rich in quartz, plagioclase, mica, and graphite with garnet porphyroblasts. Other minerals of minor abundance include calcite, zircon, iron oxides, and pseudomorphs of chlorite and epidote after amphibole and plagioclase porphyroclasts. At Iyokrok, schists with plagioclase-quartz-biotite-garnet \pm muscovite \pm staurolite(?) mineral assemblages were reported (Boak et al., 1987). These assemblages most likely have sedimentary protoliths with low abundances of Al and K (little to no muscovite). Similar clay-rich sandstones, siltstones, and silica-rich claystones are documented in the Etivluk Group of the distal Arctic Alaska passive margin (Mayfield et al., 1983).

3. Greenschists. Greenschist-facies metamorphic rocks structurally underlie and are tectonically intermixed with amphibolites of the upper metamorphic sole. The basal contact of the metamorphic sole is transitional in places where greenschists grade in broken succession into underlying unmetamorphosed sequences. Banded schists and phyllites, similar to those interlayered with amphibolite, constitute the upper part of the greenschists. The intermixing is interpreted as a function of postmetamorphism faulting. The bulk of the schists have mineral assemblages of quartz-plagioclase-biotite \pm garnet-chlorite-pyrite (metasediments) or plagioclase-quartz-actinolite-chlorite \pm garnet \pm calcite \pm magnetite (metabasites). Metamorphic grade decreases structurally downward where banded schists grade into, and are locally mixed with, chlorite-epidote-actinolite-albite metavolcanics with decreasing degrees of recrystallization and increasing prominence of relict igneous mineral phases (clinopyroxene and plagioclase) and textures. Metasedimentary rocks include recrystallized radiolarian chert, fossiliferous marble, argillite, shale, and tuff.

Metamorphic textures in greenschists are dramatically influenced by original textures and grain size. Mylonitic fabrics, like those described above for amphibolite, are most common in rocks near the top of the greenschists. In underlying lower grade rocks, effects of dynamic metamorphism are less common and more localized. Original textures are generally preserved in units with limited dynamic recrystallization. Thermal metamorphism

of these units produces blasto-interstitial, blasto-ophitic, and blasto-porphyritic recrystallized primary igneous textures. Relict pyroxenes commonly have actinolitic overgrowths and plagioclase is albitized and clouded by clay inclusions. Rocks with finer grained original textures are more recrystallized than adjacent coarser grained ones.

Unmetamorphosed Copter Peak volcanic and sedimentary rocks most commonly underlie the greenschist unit. Etivluk Group pelagic material, melange, and broken formation are also found at Misheguk and Siniktanneyak. Locally these units form gradational contacts with the overlying metamorphic sole. Although disrupted by faults, some contacts are gradual enough to trace a single unit into the metamorphic sole. The best example is the transition from greenschist to albite-actinolite hornfels to unmetamorphosed Copter Peak tholeiite exposed along traverses 7, 8, 9, and 11 (Fig. 2). These relations indicate that the protolith for the greenschist-facies metavolcanic rocks and intercalated sedimentary material is locally stratigraphically linked to the Copter Peak allochthon and Etivluk Group pelagics, which presently structurally underlie the Brooks Range ophiolite and its metamorphic sole.

Whole-rock geochemistry

Whole-rock geochemical analyses were conducted to test compositional similarities between rocks of the metamorphic sole and possible protolith units and to provide some constraints for the tectonic affinity of these units (Table 2). Major and rare earth elements were analyzed by inductively coupled plasma emission spectrometry (ICP) by methods of Walsh (1980) and Walsh et al. (1981). SiO₂ was determined by the methods of Shapiro and Brannock (1962). Other trace elements and some rare earth elements (REE) were analyzed with x-ray fluorescence (XRF) using methods similar to those of Thirwall and Burnard (1990).

The abundance of "immobile" trace elements and REE in amphibolite schists is very similar to that in mafic igneous material of the Copter Peak allochthon (Fig. 6). MORB-normalized immobile trace element abundances of mafic schists mimic the enriched N-type MORB trends of Copter Peak allochthon transitional tholeiites, which are shaded in Figure 6A. Mafic schist Y/Nb ratios (3.6–2.1, 2.55 ave.) and TiO₂ wt% (1.46 ave.) are also similar to the transitional tholeiite group of Copter Peak allochthon lava compositions. REE abundances in the mafic schists are also akin to more transitional-type lavas (Ce/Yb of 1.8–7.2) with slightly enriched LREE patterns (shaded in Fig. 6B). In general, the most immobile element abundances of mafic schists in the metamorphic sole overlap with those of Copter Peak allochthon lavas; both have transitional tholeiite compositions.

Mineral chemistry

Routine microprobe analyses of metamorphic minerals were conducted to provide temperature/pressure and protolith constraints. Minerals analyzed include amphibole, feldspar, garnet, mica, epidote, chlorite, sphene, and relict grains. The minerals were analyzed at University College of London using a

Cambridge Instruments Microscan V electron microprobe with a Link System energy dispersive system. Natural silicates and pure metals were used for standards.

Garnet. Almandine garnet is present but not abundant in most medium-grade metamorphic rocks within 50 m of the Brooks Range ophiolite contact. The crystals commonly occur as less than 0.8 mm idioblastic grains with inclusion-rich cores. Some inclusion trails are S-shaped and, along with snowball garnets, indicate synkinematic growth (Fig. 5 and 6). The geometry of inclusions within garnet cores are commonly discordant to fabrics encompassing the grains. This may be a function of static fabric development after garnet rotation or rotation not accompanied by garnet growth.

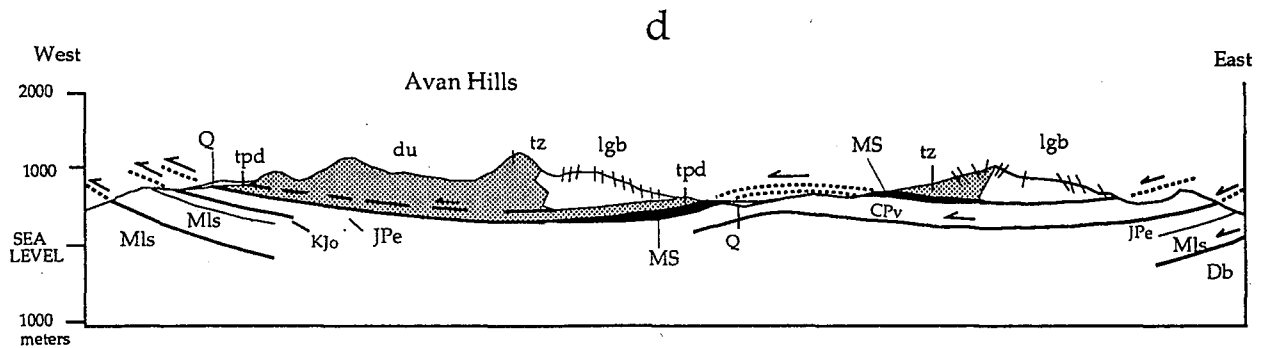
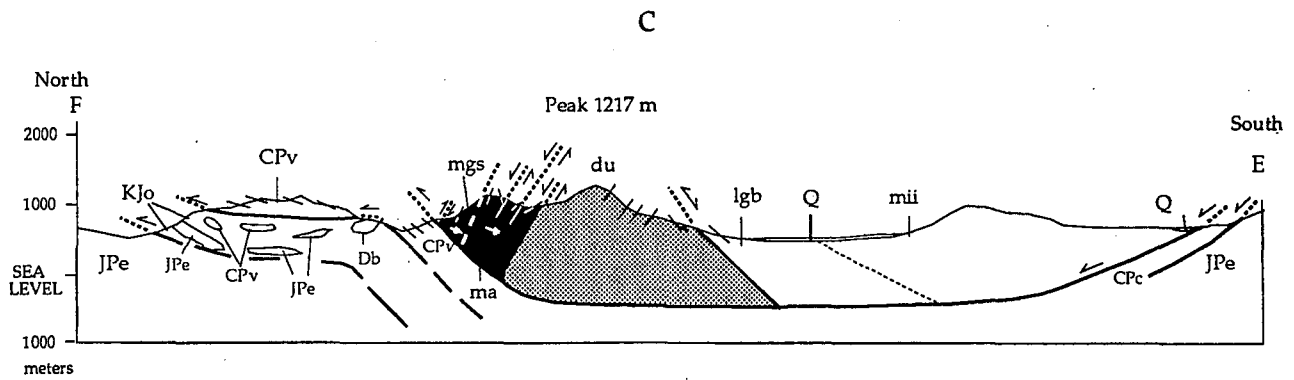
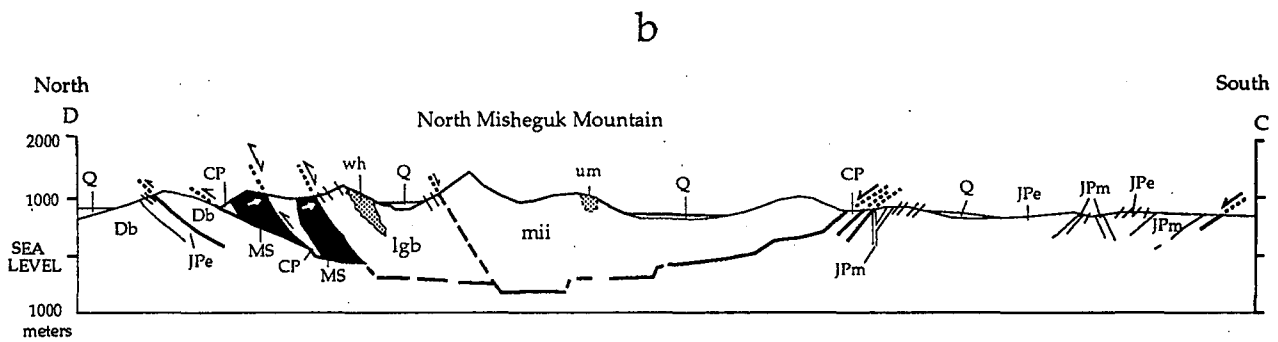
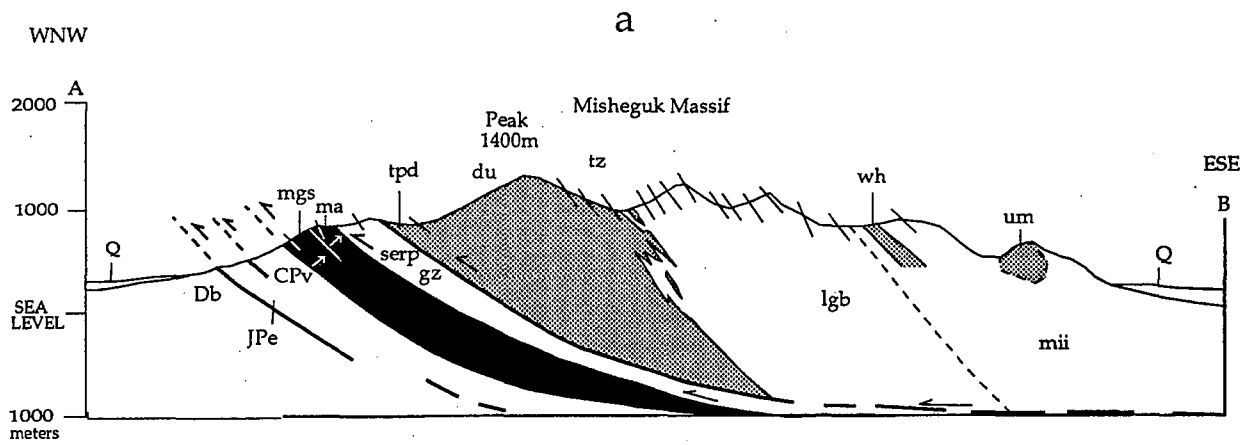
Garnet composition varies at a crystalline scale (core to rim of zoned crystals) and with distance from the Brooks Range ophiolite contact (Table 3). Almandine-rich garnet of Alm 60.5–62.3, Sp 5.5–6.7 and Pyr 27.2–30.0 is found in metagabbro 3 m above the basal fault contact of the ophiolite along traverse 1. At the emplacement fault contact garnets are typically reversely zoned with an increase in spessartine toward crystal rims. Below the fault, garnet has prograde zoning patterns (spessartine-rich cores) and exhibit an increase in Mn from Sp 17.8 to Sp 24.3 and decrease in Mg from Pyr 12.9 to Pyr 4.9 with increasing distance from the contact. The presence of garnet throughout the metamorphic sole is strongly controlled by rock chemistry, particularly layers rich in Mn (traverse 11, Table 1).

Amphibole. Amphibole compositions vary systematically throughout the metamorphic sole and within individual samples. In the upper section of the metamorphic sole poikiloblastic porphyroblasts 0.5–2.2 mm in diameter of magnesio- and tschermakitic-hornblende are mantled by smaller neoblasts of actinolitic- and magnesio-hornblende. Si and Ti cation abundances (23 oxygen basis), which reflect grade of metamorphism (Raase, 1974; Miyashiro, 1975), indicate porphyroblasts formed at lower amphibolite facies (6.40–6.72 Si and 0.09–0.13 Ti) and neoblasts at greenschist-amphibolite transition facies (6.93–7.30 Si and 0.03–0.07 Ti). The reverse of this trend is found in the underlying greenschists and epidote-amphibolites: fine-grained, foliation-forming amphiboles are usually a higher temperature variety (6.67–6.90 Si and 0.05–0.08 Ti) than amphibole porphyroblasts that are actinolitic.

Amphibole compositions provide only general constraints for interpreting the pressure and temperature of metamorphism. Pressure-sensitive relations of Al^{vi} to Si and Al^{iv} in metamorphic



Figure 3. Structural cross sections through the Brooks Range ophiolite at Misheguk Mountain and Avan Hills. Positions of lines A–B and C–D are shown in Figure 2. Line through Peak 1217m is at east edge of Figure 2 near traverse 12. East-west line through Avan Hills is field modified from Curtis et al. (1984). Surface dip is shown by lines intersecting the topographic surface: these lines indicate dip directions of various planar structural markers (magmatic flow fabric in ophiolite, foliation planes in metamorphic sole, and bedding planes in subophiolite thrust sheets). Metamorphic sole is black with arrows indicating direction of increasing metamorphic grade. Ultramafic portions of ophiolite are shaded. Abbreviations are as in Figure 2.



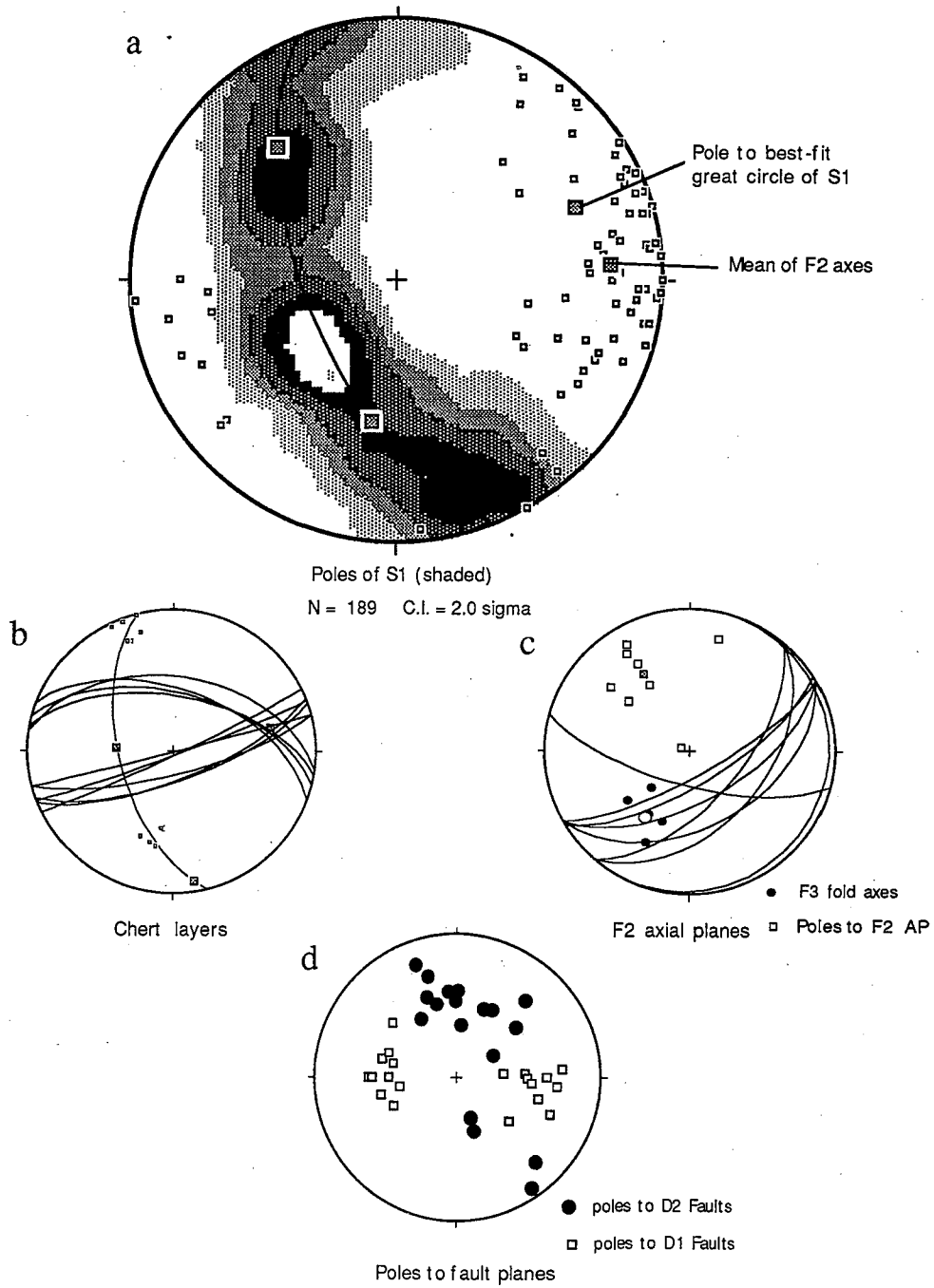


Figure 4. Lower hemisphere equal-area stereographs of structural features in the metamorphic sole. a, shaded contours of poles to S1 foliation planes (Kamb contour method) and F2 fold axes (small open squares). Pole to best-fit great circle of S1 foliation (large open circle) is near mean direction of F2 axes (large shaded square). b, Folded chert layers in transition between lower greenschist-facies metamorphic sole and the Copter Peak complex. Bedding planes are shown as great circles and poles to planes. Fold orientation is similar to foliation planes of Figure 4A. c, F2 axial planes plotted as great circles and poles to planes with F3 fold axes. Mean directions of poles to F2 axial planes are shown in shaded square, and open circle for F3 fold axes. d, Poles of fault planes in the metamorphic sole. Faults associated primarily with D1 were most likely near horizontal before folding along a north-south axis. Faults associated with D2 dominantly dip south.

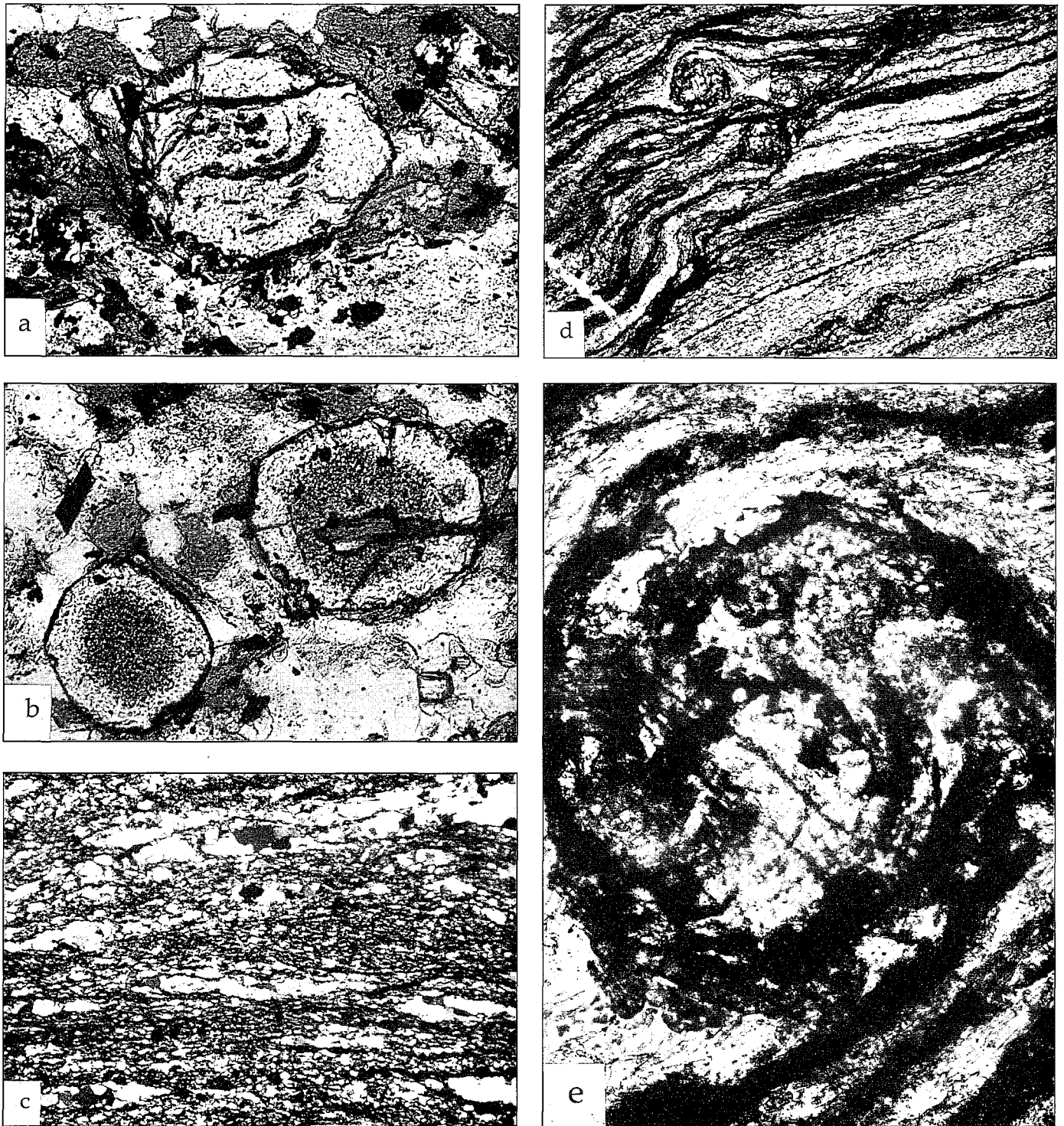


Figure 5. Photomicrographs of microstructures of the metamorphic sole related to synkinematic growth indicators in quartz-mica schist. a, Helicitic garnet with curved inclusion of previous foliation (0.5 mm field of view). b, Idioblastic garnets indicative of late static crystal growth (0.5 mm field of view). c, Polycrystalline quartz ribbons with polygonized subgrains in polarized light (3 mm field of view). Quartz ribbon characteristics mostly fit the type 2A classification of Boullier and Bouchez (1978). Locally a grain shape preferred orientation of type 2B occurs. d, Snowball garnet with graphitic bands. Layer-parallel S1 foliation is disrupted by F2 folds and postmetamorphic shear and tension fractures (3 mm field of view). e, Detail of snowball garnet in A'' (0.5 mm field of view).

TABLE 2. METAMORPHIC SOLE WHOLE-ROCK CHEMISTRY

Sample	73	79	80	115	124a	124b	132b	134a	150	154	170b
Major Elements											
SiO ₂	47.48	47.81	48.36	46.73	46.21	46.39	47.62	50.62	45.26	42.64	44.99
TiO ₂	1.80	1.84	1.87	2.56	1.26	1.23	1.26	1.01	0.65	0.92	0.11
Al ₂ O ₃	14.32	14.61	13.65	13.41	13.06	13.95	15.54	17.16	12.37	15.53	2.74
FeO	8.79	7.91	0.82	7.04	6.37	5.90	8.84	6.19	3.70	3.37	2.61
Fe ₂ O ₃	2.55	4.64	4.57	7.80	5.44	5.43	2.85	2.57	1.18	4.98	3.19
MnO	0.17	0.16	0.17	0.21	0.17	0.24	0.40	0.15	0.11	0.13	0.11
MgO	8.57	7.17	7.09	6.30	7.10	7.21	8.61	5.96	3.29	5.70	25.91
CaO	10.42	11.41	10.09	8.31	16.84	14.81	7.51	6.61	14.85	15.01	12.64
Na ₂ O	2.19	2.34	2.87	4.01	0.80	1.48	2.62	5.31	0.42	2.08	0.07
K ₂ O	0.41	0.41	0.67	0.18	0.41	0.48	1.13	0.11	2.37	0.70	0.00
P ₂ O ₅	0.17	0.16	0.15	0.23	0.14	0.18	0.23	0.12	0.12	0.13	0.03
LOI	3.09	2.06	1.47	3.31	1.64	2.11	2.94	4.47	15.67	7.99	6.98
Total	99.96	100.52	99.78	100.09	99.48	99.41	99.55	100.28	99.99	99.18	99.38
Trace Elements											
Li	17	8	9	14	0	44	28	39	60	17	2
Sc	41	44	43	43	41	40	31	32	14	35	55
Ti	10791	11031	11211	15347	7554	7374	7554	6055	3897	5515	659
V	315	337	353	434	233	300	260	247	115	216	139
Cr	293	313	120	77	234	245	313	59	70	164	1298
Co	45	55	56	52	59	65	60	41	24	46	57
Ni	104	130	79	76	86	86	230	66	62	87	513
Cu	145	118	56	238	10	92	16	30	24	41	6
Zn	93	94	97	123	96	89	129	80	88	73	34
Rn	12	12	14	6	10	12	24	5	112	15	0
Sr	194	194	202	105	330	172	317	410	253	217	8
Y	23	23	26	33	21	21	34	18	23	15	2
Zr	58	25	16	36	32	24	49	25	113	24	5
Nb	10	10	11	13	10	10	11	5	13	9	6
Ba	169	224	608	75	121	158	903	202	446	142	7
REE											
La	7.60	12.20	13.50	9.60	13.40	13.00	34.10	11.20	27.70	10.90	1.30
Ce	17.70	15.70	17.80	25.20	13.00	11.80	49.30	11.60	56.20	8.60	0.20
Pr	2.60	2.60	2.80	3.80	2.00	1.90	6.40	2.10	7.00	1.50	0.10
Nd	12.80	12.00	12.90	17.50	9.20	9.10	26.10	9.90	26.20	6.70	0.50
Sm	3.60	3.40	3.80	5.00	2.80	2.70	6.10	2.90	5.50	2.00	0.20
Eu	1.30	1.30	1.40	1.80	1.10	1.10	1.60	0.90	1.20	0.80	0.10
Gd	4.50	4.70	4.80	6.40	3.60	3.80	6.60	3.20	5.00	2.60	0.30
Dy	4.60	4.60	5.00	6.60	4.00	4.20	6.40	3.50	4.30	2.80	0.40
Ho	0.90	0.90	1.10	1.40	0.80	0.90	1.30	0.70	0.90	0.60	0.10
Er	2.60	3.00	3.00	3.80	2.50	2.30	3.90	2.30	2.50	1.70	0.30
Yb	2.10	2.20	2.60	3.00	2.20	1.00	3.20	2.00	2.20	1.50	0.20
Lu	0.30	0.30	0.40	0.40	0.40	0.10	0.50	0.40	0.30	0.20	0.00

amphiboles (Raase, 1974; Fleet and Barnett, 1978) indicate pressures for the entire metamorphic sole of around or slightly above 5 Kb. Ti-rich amphiboles increase in abundance upward toward the Brooks Range ophiolite contact. This trend is most likely a function of increased temperature rather than compositional variation, due to the presence of other coexisting Ti-bearing phases like sphene and ilmenite.

Plagioclase. Plagioclase occurs throughout the metamorphic sole as 0.5–2.0 mm porphyroblasts and less than 0.5 mm xenoblastic grains. Original plagioclase compositions, particularly of porphyroblasts, are difficult to determine due to secondary effects of albitization and alteration to cloudy aggregates of

white mica, epidote and clays. Least altered parts of plagioclase grains show some compositional variation with distance from the Brooks Range ophiolite contact. More calcic plagioclase of An (46–24) is found within 20 m of the Brooks Range ophiolite contact, although the range overlaps with that of plagioclase found 20–50 m from the contact (An 36–25). Late albite is present in most samples and is commonly associated with prehnite in veins that truncate all other deformational fabrics.

Geothermometry

Geothermometric estimates were obtained using coexisting phases of garnet, amphibole, and biotite. High Mn contents in

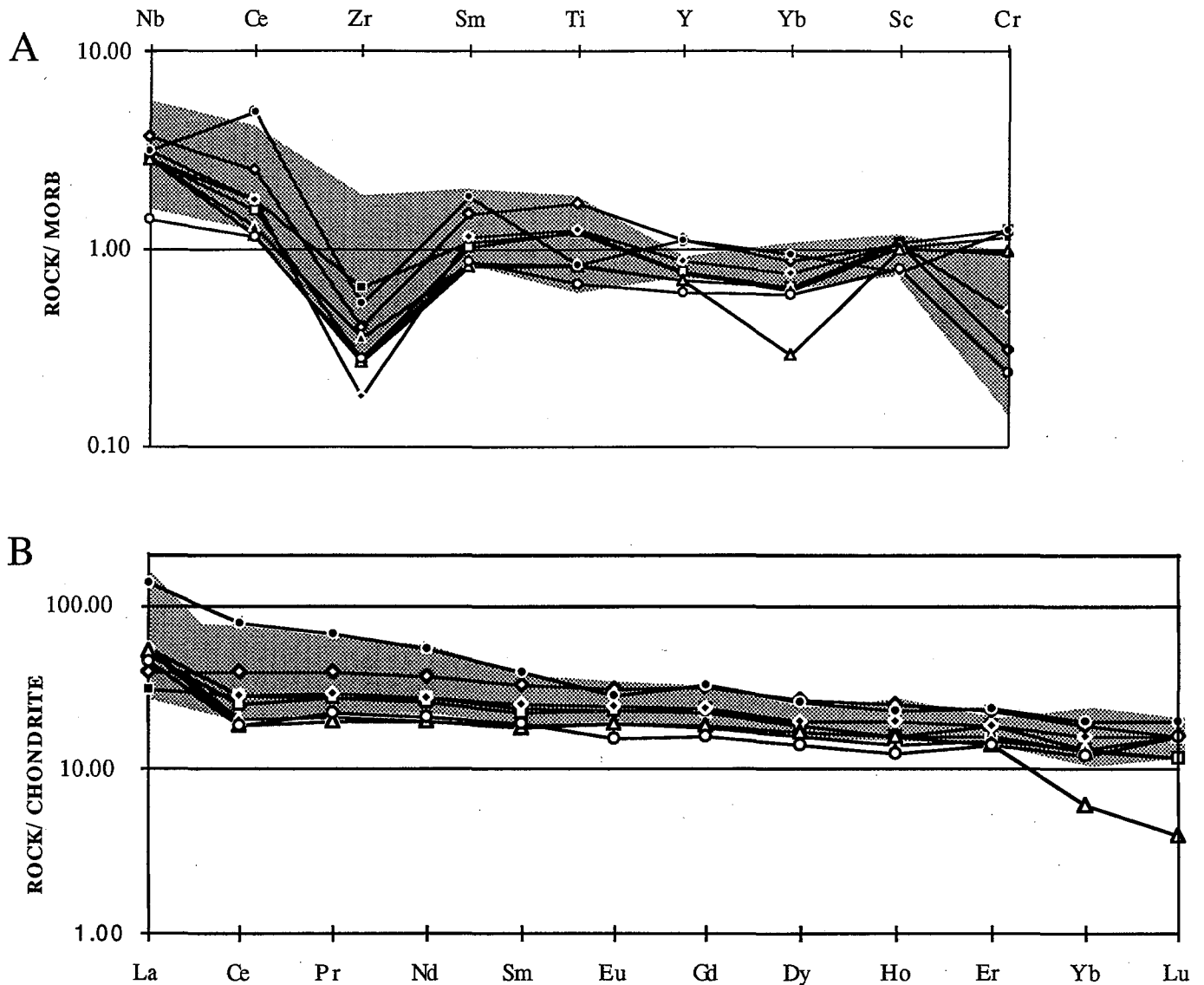


Figure 6. Geochemical comparison between metamorphic sole mafic schist (metabasalt) and Copter Peak basalt (shaded). A, MORB-normalized trace element abundances. B, chondrite-normalized REE abundances. Shaded area is trend of eight Copter Peak basalt analyses. Trends are consistent with T-Type MORB lavas.

most garnets (12.0 mole % average with values as much as 24.3 mole %) precluded obtaining estimates from most of the metamorphic units. The 5-Kb pressure estimate obtained from relations of Alvi to Si and Aliv in metamorphic amphiboles (Raase, 1974; Fleet and Barnett, 1978) was assumed for the geothermometric model. Chemical analysis of homogenous pairs of low-Mn garnet and biotite from a metapelite 40–50 m below the ophiolite were used with TWEEQU thermobarometry software (Berman, 1991) to yield temperature estimates of 550°C. The mixing models of Berman (1990) for garnet and McMullin et al. (1991) for biotite account for nonideal behavior in the solid solutions. Coexisting phases of low-Mn garnet and amphibole were also used from mylonites 4–5 m below the structural base of the

ophiolite. These rocks yield temperature estimates of 500–560°C using the garnet-hornblende geothermometer of Graham and Powell (1984).

Boak et al. (1987) estimated temperatures of 560°C for a garnet rim–biotite pair in amphibolite below the Brooks Range ophiolite at Iyokrok. This estimate applies only to the medium-grade metamorphic rocks “a few tens of meters” from the ophiolite contact. Partial melts of material thrust beneath the Brooks Range ophiolite at Avan Hills and Siniktanneyak indicate that local temperatures along the base of the ophiolite must have been greater than 650°C, which is the intersection between the 5-Kb line and the melting curve for water-saturated peraluminous granite (Clemens and Wall, 1981).

Compositional variation in mineral chemistry between the low- to medium-grade and higher grade metamorphic mineral assemblages (systematic changes in plagioclase, hornblende, and garnet composition upward) indicate a general increase in metamorphic grade upward toward the base of the Brooks Range ophiolite. However, the detailed thermal evolution of the "inverted" metamorphic sequence is unclear. The occurrence of retrograde metamorphism and metasomatism only in the highest

grade rocks nearest the ophiolite contact, and the presence of blocks of amphibolite within greenschists, suggest the amphibolite unit may have formed before the lower grade rocks it now overlies. It is also possible that mixing may have resulted entirely from post-peak metamorphism faulting.

Age of metamorphism

K-Ar and $^{40}\text{Ar}/^{39}\text{Ar}$ radiometric age analyses were conducted on hornblende from garnet amphibolite collected 5 m below the emplacement thrust of the Brooks Range ophiolite at Misheguk. Hornblende and plagioclase layers comprise most of the rock in equal amounts with minor garnet and sphene. Compositional layers are disrupted by veins associated with retrograde mineral assemblages (epidote + chlorite + white mica + albite). Porphyroblasts (as large as 1.2 mm) of magnesio- and tschermakitic-hornblende are locally mantled with smaller neoblasts of magnesio-hornblende, which are more enriched in Si and depleted in Ti than the porphyroblasts. Plagioclase porphyroblasts range in composition from An 28 to An 38 and are commonly saussuritized. Almandine garnet with Mn-rich rims is distributed unevenly in the sample and is most closely associated with chlorite- and white mica-rich layers. The low Fe content of the hornblende renders it most suitable for $^{40}\text{Ar}/^{39}\text{Ar}$ dating (O'Nions, 1969).

Hornblende from sample 132b (Table 2) yields an $^{40}\text{Ar}/^{39}\text{Ar}$ plateau age of 165 ± 3 Ma (Fig. 7). This age is similar to other plateau ages of 164–169 Ma of hornblende from the structural base of Avan Hills and 163–171 Ma at the base of the Asik (Wirth et al., 1987). These ages are significantly older than hornblende K/Ar ages from the sample 132 (157 ± 5 Ma) at Misheguk and those reported from Iyokrok of $153\text{--}154 \pm 5$ Ma by Boak et al. (1987). Age discrepancies between hornblende separates, some from the same sample, may be due to difficulties of the K-Ar method in (1) estimating the small amounts of K present in the amphiboles used and (2) detecting Ar loss.

Cooling ages from the metamorphic sole are concordant with hornblende $^{40}\text{Ar}/^{39}\text{Ar}$ plateau ages from high-level gabbro and diorite at Misheguk (Harris, 1998), Asik, and Avan Hills (Wirth and Bird, 1992) of 163–171 Ma. Plagiogranite from Siniktanneyak yielded a U-Pb age of 170 ± 3 Ma (Moore et al., 1993). These ages are also concordant with a white mica $^{40}\text{Ar}/^{39}\text{Ar}$ Ar plateau age of 171 ± 4 Ma from Ruby Ridge in the metamorphic core of the Brooks Range (Christiansen and Snee, 1994). Age concordance may be associated with a common tectonic uplift event that cooled both the igneous and metamorphic rocks of the Brooks Range ophiolite and the continental material beneath them. An alternative explanation may be that conductive cooling of the ophiolite slab coincided with high pressure metamorphism in the Schist belt.

The cooling history of subophiolite metamorphic rocks has implications for the tectonic processes and uplift rates associated with ophiolite emplacement. $^{40}\text{Ar}/^{39}\text{Ar}$ age data from metamorphic minerals with different closure temperatures provide independent time-temperature control points that help constrain the timing of

TABLE 3. GARNET COMPOSITIONS*

Number	Distance	Alm	Gro	Py	Sp	C/R
78.1	1m	0.619	0.034	0.280	0.067	-
78.2		0.614	0.048	0.281	0.057	-
78.3		0.623	0.049	0.272	0.055	-
78.6		0.605	0.033	0.300	0.062	-
78.7		0.613	0.051	0.280	0.057	-
78.8		0.618	0.034	0.289	0.060	-
83A.3	1m	0.357	0.214	0.028	0.401	C
83A.5		0.340	0.275	0.000	0.385	Micro
83A.7		0.539	0.204	0.086	0.170	-
83A.8		0.402	0.336	0.016	0.247	C
83A.9		0.547	0.246	0.038	0.168	R
132SP.1	4-5m	0.619	0.075	0.129	0.178	C
132SP.2		0.395	0.099	0.222	0.284	Int
132SP.3		0.626	0.061	0.125	0.187	R
132SP.9		0.649	0.044	0.136	0.649	Micro
132B.1		0.537	0.126	0.199	0.138	C
132B.1		0.555	0.121	0.164	0.159	R
132B.2		0.488	0.210	0.159	0.143	C
132B.2		0.535	0.167	0.168	0.130	R
132B.3		0.560	0.153	0.195	0.091	C
132B.3		0.547	0.160	0.194	0.098	R
9C.3	10m	0.535	0.172	0.028	0.265	-
9C.8		0.491	0.156	0.023	0.329	C
9C.9		0.531	0.157	0.035	0.277	R
9C.10		0.498	0.161	0.000	0.341	C
9C.11		0.515	0.166	0.032	0.288	R
9C.15		0.529	0.170	0.029	0.271	C
9C.17		0.540	0.175	0.034	0.251	R
150DP.1	20-50m	0.663	0.086	0.051	0.201	C
150DP.5		0.508	0.215	0.034	0.243	C
150DP.13		0.591	0.164	0.049	0.196	Inc. in 14
150DP.14		0.616	0.120	0.045	0.218	C
150DP.14		0.707	0.070	0.073	0.150	R
123B.1a	30-50m	0.589	0.073	0.085	0.253	Int
123B.1b		0.652	0.063	0.100	0.184	C
123B.1c		0.593	0.072	0.081	0.255	R
123B.2a		0.511	0.087	0.065	0.336	C
123B.2b		0.577	0.083	0.070	0.270	Int
123B.2c		0.645	0.063	0.093	0.199	R
123B.3a		0.548	0.084	0.065	0.304	C
123B.3b		0.602	0.067	0.081	0.249	Int
123B.3c		0.649	0.070	0.092	0.190	R
123B.15a		0.554	0.175	0.076	0.195	R

*Alm = Almandine; Gro = grossularite; Py = pyrope; Sp = spessartine; C/R = core/rim; Micro = small grain; Int = intermediate between C/R; Inc. = inclusion.

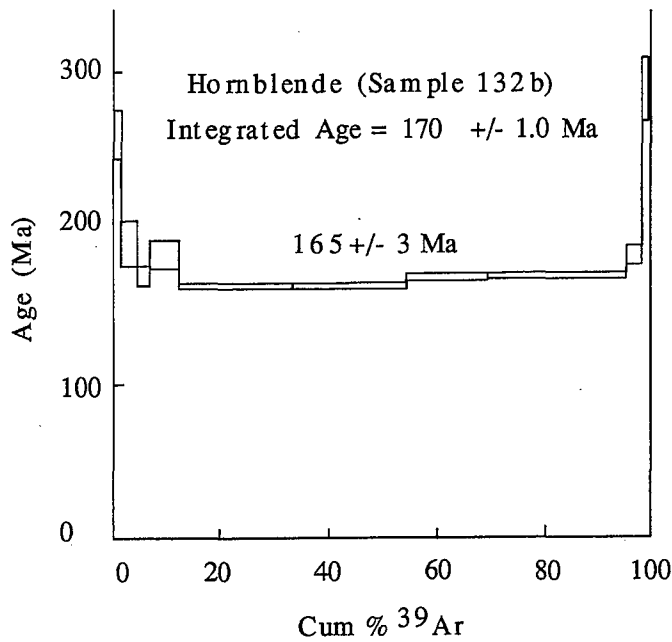


Figure 7. $^{40}\text{Ar}/^{39}\text{Ar}$ age spectra for hornblende from sample 132b (traverse 7 at 4–5 m below the structural base of Brooks Range ophiolite). Plateau age has slight saddle-shaped spectrum, which may be a function of excess argon in unstable sites within the mineral grains.

various pressure-temperature metamorphic conditions. Age spectra from $^{40}\text{Ar}/^{39}\text{Ar}$ analyses of hornblende, biotite, and K-feldspar from the metamorphic sole of the Brooks Range ophiolite provide constraints for effective closure temperatures of these minerals. Plotting these temperatures against time yields an empirical cooling curve for subophiolite metamorphism (Harris, 1992; Wirth and Bird, 1992). Maximum temperatures for the cooling curve are provided by Ar closure temperatures for hornblende, which are mostly controlled by cooling rate, composition, and grain size. An intermediate-high cooling rate of 10–15°C/Ma is assumed for the metamorphic sole based on differences in age between subophiolite metamorphism, basement uplift, and deposition of detritus from high-pressure metamorphic rocks (Till et al., 1988). At these rates, the argon closure for hornblende is about $530 \pm 40^\circ\text{C}$ (Harrison and McDougall, 1980). The overlap of closure temperatures and geothermometric estimates from garnet-amphibole pairs within the dated sample and from garnet-biotite pairs several decimeters below the base of the ophiolite, indicate that the $^{40}\text{Ar}/^{39}\text{Ar}$ age is close to the age of metamorphism.

ORIGIN AND TECTONIC EVOLUTION

The metamorphic sole of the Brooks Range ophiolite represents the initial plate boundary suture between an arc-related upper plate and the underthrust continental margin of Arctic Alaska. The plate boundary moved to lower structural levels as the Brookian orogen progressed, which caused uplift and cooling of the metamorphic sole suture. In this process the metamorphic sole was structurally modified by postmetamorphic deformation.

However, the metamorphic sole preserves a general record of its origin, conditions of dynamothermal metamorphism, and tectonic evolution.

Exposures of the metamorphic sole have a consistent succession of garnet-bearing amphibolite and quartz-mica mylonitic schists that decrease in metamorphic grade downward into greenschist facies and unmetamorphosed protoliths. The protolith of amphibolite grade mylonite that is “welded” to the structural base of the Brooks Range ophiolite document the crustal composition of footwall rocks that first underthrust the hot ophiolite as it was detached and moved upward. Geochemical similarity between mafic amphibolites and Copter Peak allochthon basalt is interpreted as evidence that the basalt was one of the first crustal units to underthrust the ophiolite after detachment. Mn-rich garnet in pelitic material are consistent with a chert and psammitic sedimentary protolith that is abundant in the Copter Peak allochthon and Etivluk Group. Chemical, age, and stratigraphic links between the metamorphic sole and distal parts of the Arctic Alaska continental margin indicate that the Brooks Range ophiolite was formed and emplaced very near to the continental margin.

Boudier and Nicolas (1988) propose a “compressed” spreading ridge tectonic model for the detachment of Oman-type ophiolites. If the Brooks Range ophiolite and other ophiolites formed at a spreading ridge that overthrust itself, metamorphic soles would be composed of rocks similar in composition and age to the ophiolites. However, differences in geochemistry and age between ophiolite and metamorphic sole rule out this tectonic scenario for the Brooks Range.

A more likely scenario that is consistent with geochemical, structural, and petrologic data is that the Brooks Range ophiolite formed above a young subduction zone that developed near the Arctic Alaska continental margin (Fig. 8). As the continental margin was pulled into the subduction zone it underthrust the hot ophiolite (young arc). Thrust stacking beneath the leading edge of the ophiolitic upper plate may have been what caused the ophiolite to detach from its roots, forming a passive roof thrust above the developing orogen.

Strain associated with the structural emplacement of the Brooks Range ophiolite was localized in the metamorphic sole, where strain rates may have been as much as 10^{-10} s^{-1} to 10^{-9} s^{-1} . Ductile strain produced blastomylonitic fabrics where crystal plastic flow was locally overprinted by thermal annealing. Flow stress estimates, based on progressive quartz subgrain size reduction, yield a stress gradient of 2–3 MPa/m in the metamorphic sole.

Temperature sensitive chemical changes in plagioclase, amphibole, and garnet overgrowths indicate that metamorphic grade increases upward toward the ophiolite. Variations in prograde and retrograde patterns exist. Most crystal growth was synkinematic at temperatures near that predicted for hornblende Ar retentivity. Geothermometric estimates from garnet-bearing amphibolite near the ophiolite yield minimum temperatures of 500–560°C. These temperatures are consistent with the type of crystal plastic deformational mechanisms (dislocation glide and

creep) observed in microstructures. Assuming an initial thickness of around 500–600m, from amphibolite-grade schist to unmetamorphosed basalts, a minimum thermal gradient of 500–600°C/km is predicted. This estimate does not take into account the higher temperatures necessary (650–700°C) to produce partial melts along the base of the ophiolite, which approach the maximum static temperature for contact metamorphism.

An estimate of the maximum temperature attainable by linear flow from a hot hanging wall of peridotite ($T^h=1,100\text{--}1,200^\circ\text{C}$) into a cool footwall ($T^f=0\text{--}100^\circ\text{C}$) is given by $0.5(T)$, where $T = T^h - T^f$ (Jaeger, 1961; Spray, 1984). Applying this constraint to probable conditions at the base of the ophiolite yields maximum temperatures of 500–600°C, which are not high enough to produce partial melts. Frictional heating may account for some excess heat, but its input is limited by the low strength of the hot hanging wall and weak material in the footwall (Spray, 1984). Another possible explanation are the “iron board” models proposed by Pavlis (1986) and Smith (1988). These models account for the interplay of thermal and mechanical processes associated with a hot, moving ophiolite slab over wet upper crustal material. The models predict that preheating, either of the footwall or hanging wall by the leading edge of the slab can raise temperatures an additional 200°C and cause local melting. Each viable model is constrained by the temperatures recorded in the metamorphic sole, which limits the time available for the Brooks Range ophiolite to cool before coming into contact with the Copter Peak allochthon to a few million years.

The inverted metamorphic gradient, overlap between ages of ophiolite cooling and subophiolite metamorphism, and structural and petrologic associations indicate that the metamorphic sole formed during tectonic emplacement of the Brooks Range ophiolite while it was still hot over mafic igneous and sedimentary rocks of the Copter Peak allochthon and perhaps other continental margin units. The timing of this event (164–169 Ma) provides a minimum age for ophiolite genesis and maximum age for the

initiation of the western Brookian orogen. The development of the metamorphic sole during ophiolite emplacement documents the thermal and mechanical conditions of the event. The narrow time and temperature windows between ophiolite genesis and emplacement, implies limited travel; that the Brooks Range ophiolite was near its birth place at the time of subophiolite metamorphism and tectonic emplacement. The general synchronicity between cooling ages of the ophiolite and its metamorphic sole is a common feature of many Oman-type ophiolites (Spray, 1984). This feature is a characteristic of ophiolite genesis by pericollisional extension (Harris, 1992).

Incorporation of the Brooks Range ophiolite and Copter Peak allochthon into the Brookian fold-thrust zone resulted in cooling of the metamorphic sole. This event coincided with the first evidence of north-directed orogenic (Brookian) sedimentation (Mayfield et al., 1983) and of metamorphism associated with the orogen (Christiansen and Snee, 1994; Gottschalk and Snee, this volume, Chapter 13). The transition from ductile to more brittle deformation mechanisms follow within 5–10 m.y. of peak-metamorphism as evidenced by the cooling ages of mica schists in the metamorphic sole (Wirth and Bird, 1992). Continental underthrusting beneath the ophiolite produced a hinterland belt of high-pressure blueschists that was subsequently overprinted by a greenschist-grade event. Metamorphic cooling occurred from 130 to 100 Ma (Armstrong et al., 1986; Gottschalk, 1990; Christiansen and Snee, 1994; Gottschalk and Snee, this volume, Chapter 13).

Uplift and unroofing of the hinterland Schist belt may be responsible for postemplacement fragmentation and remobilization of the Brooks Range ophiolite nappe and its metamorphic sole. This event is documented by the fault juxtaposition of amphibolite with greenschist-facies rocks within the metamorphic sole, and the stacking of these rocks above continental margin sedimentary rocks with conodont alteration values of only 1–2 (Harris, A. G., et al., 1987). The final phase of brittle deformation recorded by the metamorphic sole may be associated with strike-slip faulting.

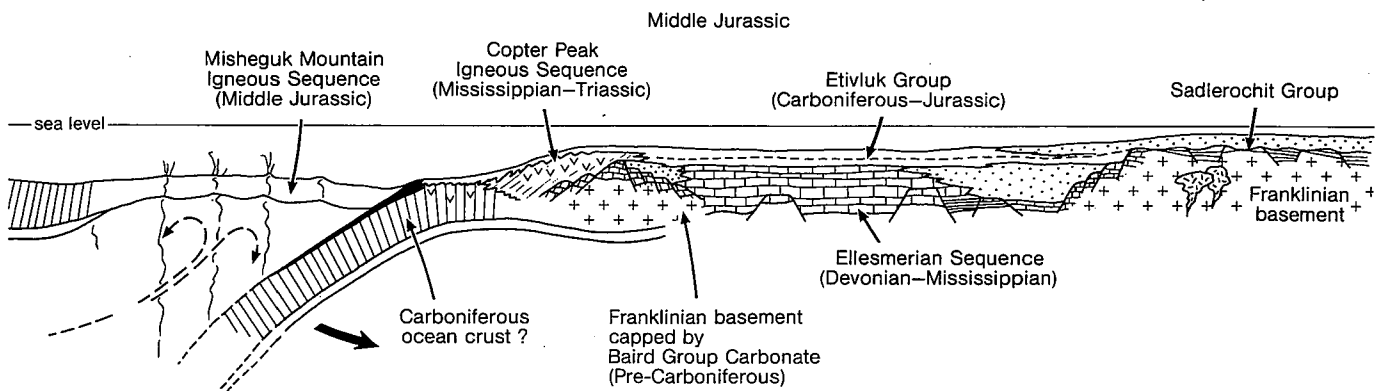


Figure 8. Middle Jurassic schematic reconstruction of the Arctic Alaska passive continental margin. The Misheguk Mountain Igneous Sequence becomes the Brooks Range ophiolite as the Brookian continental margin is thrust beneath it. The Copter Peak Igneous Sequence is interpreted in part to represent a rift-related volcanic pile similar to many other volcanic margins (see Mutter et al., 1988). The width of the intracratonic basin sequence is underestimated for illustration purposes. The dashed line marks the breakup unconformity.

ACKNOWLEDGMENTS

Support for this research was provided by grants from the American Chemical Society–Petroleum Research Fund, U.S. Geological Survey, U.S. Bureau of Mines, and the Rice University/University of Alaska Industrial Research Program. I wish to thank Mike Audley-Charles, Robert Hall, Helen Lang, Roger Mason, Mike Searle, and David Stone for direction and encouragement. Cal Wescott, Jeff Foley, and Tom Light provided field support. Paul Ballantyne and J. Walsh assisted with whole-rock geochemical analyses. Dengliang Gao assisted with piezometric measurements. Helen Lang, Rick Gottschalk, Jay Zimmerman, Aley El-Shazly, and Brian Patrick provided careful reviews of various drafts of the manuscript. Access to the Noatak Wilderness was granted by the U.S. Park Service.

REFERENCES CITED

- Alexander, R. A., 1990, Structure and lithostratigraphy of the Kikiktat Mountain area, central Killik River Quadrangle, north-central Brooks Range, Alaska [M.A. thesis]: Fairbanks, Alaska, University of Alaska, 248 p.
- Armstrong, R. L., Harakal, J. E., Forbes, R. B., Evans, B. W., and Thurston, S. P., 1986, Rb-St and K-Ar study of the metamorphic rocks of the Seward Peninsula and southern Brooks Range, Alaska, *in* Evans, B. W., and Brown, E. H., eds., Blueschists and eclogites: Geological Society of America Memoir 164, p. 185–203.
- Barker, F., Jones, D. L., Budahn, J. R., and Coney, P. J., 1988, Ocean plateau-seamount origin of basaltic rocks, Angayucham Terrane, central Alaska: *Journal of Geology*, v. 96, p. 368–374.
- Berman, R. G., 1990, Mixing properties of Ca-Mg-Fe-Mn garnets: *American Mineralogist*, v. 75, p. 328–344.
- Berman, R. G., 1991, Thermobarometry using multiequilibrium calculations: a new technique, with petrologic applications: *Canadian Mineralogist*, v. 29, p. 833–855.
- Boak, J. L., Turner, D. L., Henry, D., Moore, T. E., and Wallace, W. K., 1987, Petrology and K-Ar ages of the Misheguk igneous sequence: An allochthonous mafic and ultramafic complex and its metamorphic aureole, western Brooks Range, Alaska, *in* TAILLEUR, I., and WEIMER, P., eds., Alaskan North Slope geology: Society of Economic Paleontologists and Mineralogists, Pacific Section, Publication 50, p. 737–745.
- Boudier, F., and Nicolas, A., 1988, The ophiolites of Oman: *Tectonophysics*, v. 151, 401 p.
- Boullier, A.-M., and Bouchez, J.-L., 1978, Le quartz en rubans dans les mylonites: *Bulletin de la Société géologique de France*, v. 7, p. 253–262.
- Box, W., 1985, Early Cretaceous orogenic belt in northwestern Alaska: internal organization, lateral extent, and tectonic interpretation, *in* Howell, D. G., ed., Tectonostratigraphic terranes of the Circum-Pacific region: Houston, Texas, Circum-Pacific Council for Energy and Mineral Resources Earth Science Series, v. 1, p. 137–147.
- Christiansen, P. P., and Snee, L. W., 1994, Structure, metamorphism, and geochronology of the Cosmos Hills and Ruby Ridge, Brooks Range Schist belt, Alaska: *Tectonics*, v. 13, p. 193–213.
- Clemens, J. D., and Wall, V. J., 1981, Origin and crystallization of some peraluminous (S-type) granitic magmas: *Canadian Mineralogist*, v. 19, p. 111–131.
- Coleman, R. G., 1977, Ophiolites—Ancient oceanic lithosphere?: New York, Springer-Verlag, 299 p.
- Coleman, R. G., 1984, The diversity of ophiolites: *Geologie en Mijnbouw*, v. 63, p. 141–150.
- Curtis, S. M., Ellersieck, I., Mayfield, C. F., and TAILLEUR, I. L., 1984, Reconnaissance geologic map of the southwestern Misheguk Mountain Quadrangle, Alaska: U.S. Geological Survey Open-File Report OF 82-612, scale 1:63,360.
- Dumoulin, J. A., and Harris, A. G., 1987, Cambrian through Devonian carbonate rocks of the Baird Mountains, western Brooks Range, Alaska: *Geological Society of America Abstracts with Programs*, v. 19, p. 373–374.
- Ellersieck, I., Curtis, S. M., Mayfield, C. F., and TAILLEUR, I. L., 1982, Reconnaissance geologic map of south-central Misheguk Mountain Quadrangle, Alaska: U.S. Geological Survey Open-File Report OF 82-612, scale 1:63,360.
- Fleet, M. E., and Barnett, F. L., 1978, Al^{IV}Al^{VI} partitioning in calciferous amphiboles from the Frood Mine, Sudbury, Ontario: *Contributions to Mineralogy and Petrology*, v. 16, p. 527–532.
- Ghent, E. D., and Stout, N. Z., 1981, Metamorphism at the base of the Samail ophiolite, SE Oman Mountains: *Journal of Geophysical Research*, v. 86, p. 2557–2572.
- Gottschalk, R. R., 1990, Structural evolution of the Schist belt, south-central Brooks Range, Alaska: *Journal of Structural Geology*, v. 12, no. 4, p. 453–469.
- Gottschalk, R. R., and Oldow, J. S., 1988, Low-angle normal faults in the south-central Brooks Range fold and thrust belt, Alaska: *Geology*, v. 16, p. 395–399.
- Graham, C. M., and Powell, R., 1984, A garnet-hornblende geothermometer: calibration, testing, and application to the Pelona schist, southern California: *Journal of Metamorphic Geology*, v. 2, p. 13–31.
- Harding, D. J., Wirth, J. M., Bird, J. M., and Shelton, D. H., 1985, Ophiolite emplacement, western Brooks Range, northern Alaska: *Eos (Transactions, American Geophysical Union)*, v. 46, p. 1129.
- Harris, A. G., Lane, H. R., TAILLEUR, I. L., and Ellersieck, I. F., 1987, Conodont thermal maturation patterns in Paleozoic and Triassic rocks, northern Alaska, *in* TAILLEUR, I., and WEIMER, P., eds., Alaskan North Slope geology: Society of Economic Paleontologists and Mineralogists, Pacific Section, Publication 50, p. 181–194.
- Harris, R. A., 1987, Structure and composition of sub-ophiolite metamorphic rocks, western Brooks Range ophiolite belt, Alaska: *Geological Society of America Abstracts with Programs*, v. 19, p. 38.
- Harris, R. A., 1992, Peri-collisional extension and the formation of Oman-type ophiolites in the Brooks Range and Banda arc, *in* Parsons, L. M., Murton, B. J., and Browning, P., eds., Ophiolites and their modern oceanic analogues: Geological Society of London, Special Publication No. 60, p. 301–325.
- Harris, R. A., 1995, Geochemistry and tectonomagmatic origin of the Misheguk Massif, Brooks Range ophiolite belt, Alaska: *Lithos*, v. 35, p. 1–25.
- Harris, R. A., 1998, The Brooks Range ophiolite, NW Alaska: U.S. Geological Survey Professional Paper (in press).
- Harris, R. A., Stone, D. B., and Turner, D. L., 1987, Tectonic implications of paleomagnetic and geochronologic data from the Yukon-Koyukuk basin, Alaska: *Geological Society of America Bulletin*, v. 99, p. 362–375.
- Harrison, T. M., and McDougall, I., 1980, Investigations of an intrusive contact, northwest Nelson, New Zealand—1. Thermal, chronological and isotopic constraints: *Geochimica et Cosmochimica Acta*, v. 44, p. 1985–2003.
- Jaeger, J. C., 1961, The coding of irregularly shaped igneous bodies: *American Journal of Science*, v. 259, no. 10, p. 721–734.
- Jamieson, R. A., 1986, P-T paths from high temperature shear zones beneath ophiolites: *Journal of Metamorphic Geology*, v. 4, p. 3–22.
- Jones, D. L., Silberling, N. J., Berg, J. C., and Plafker, G., 1981, Tectonostratigraphic terrane map of Alaska: U.S. Geological Survey Open-File Report 81-792, scale 1:2,500,000.
- Kretz, R., 1983, Symbols for rock-forming minerals: *American Mineralogist*, v. 68, p. 277–279.
- Kronenberg, A. K., and Shelton, G. L., 1980, Deformation microstructures in experimentally deformed Maryland diabase: *Journal of Structural Geology*, v. 2, p. 341–353.
- Martin, A. J., 1970, Structure and tectonic history of the western Brooks Range De Long Mountains and Lisburne Hills, northern Alaska: *Geological Society of America Bulletin*, v. 81, p. 3605–3622.
- Mayfield, C. F., TAILLEUR, I. L., and Ellersieck, I., 1983, Stratigraphy, structure and palinspastic synthesis of the western Brooks Range, northwestern Alaska: U.S. Geological Survey Open-File Report OF 83-779, 58 p., 5 pl.
- McMullin, D. W. A., Berman, R. G., and Greenwood, H. J., 1991, Calibration of

- SGAM thermobarometer for pelitic rocks using data from phase-equilibrium experiments and natural assemblages: *Canadian Mineralogist*, v. 29, p. 889–908.
- Mercier, J. C., Anderson, D. A., and Carter, N. L., 1977, Stress in the lithosphere; inferences from steady state flow of rocks: *Pure and Applied Geophysics*, v. 115, no. 1–2, Stress in the Earth, p. 199–226.
- Miyashiro, A., 1975, Classification, characteristics and origin of ophiolites: *Journal of Geology*, v. 83, p. 249–281.
- Moore, T. E., 1987, Geochemical and tectonic affinity of basalts from the Copter Peak and Ipnarik River allochthons, Brooks Range, Alaska: *Geological Society of America Abstracts with Programs*, v. 19, p. 434.
- Moore, T. E., and Grantz, A., 1987, Crustal structure of central Alaska along Geodynamics continent/ocean transect (A-3): *Geological Society of America Abstracts with Programs*, v. 19, p. 434.
- Moore, T. E., Aleinikoff, J. N., and Walter, M., 1993, Middle Jurassic U-Pb crystallization age for Siniktanneyak Mountain ophiolite, Brooks Range, Alaska: *Geological Society of America Abstracts with Programs*, v. 25, p. 124.
- Moores, E. M., 1970, Ultramafics and orogeny, with models for the US Cordillera and the Tethys: *Nature*, v. 228, p. 837–842.
- Moores, E. M., 1982, Origin and emplacement of ophiolites: *Reviews of Geophysics and Space Physics*, v. 20, p. 735–760.
- Moores, E. M., Robinson, P. T., Malpas, J., and Xenophontos, C., 1984, Model for the origin of the Troodos massif, Cyprus, and other mid-east ophiolites: *Geology*, v. 12, p. 500–503.
- Mull, C. G., 1982, The tectonic evolution and structural style of the Brooks Range, Alaska: An illustrated summary, in Powers, R. B., ed., *Geological studies of the Cordilleran Thrust Belt*: Denver, Colorado, Rocky Mountain Association of Geologists, v. 1, p. 1–45.
- Mutter, J. C., Buck, R. W., and Zehnder, C. M., 1988, Convective partial melting. 1. A model for the formation of thick basaltic sequences during the initiation of spreading: *Journal of Geophysical Research*, v. 93, p. 1031–1048.
- Nelson, S. W., and Nelson, W. H., 1982, Geology of Siniktanneyak Mountain ophiolite, Howard Pass Quadrangle, Alaska: U.S. Geological Survey Miscellaneous Field Studies Map MF-1441, scale 1:63,360.
- O'Nions, R. K., Smith, D. G., Baadsgaard, H., and Moreton, R. D., 1969, Influence of chemical composition on argon retentivity in metamorphic calcic amphiboles from south Norway: *Earth and Planetary Science Letters*, v. 5, p. 339–345.
- Pallister, J. S., Budahn, J. R., and Murchey, B. L., 1989, Pillow basalts of the Angayucham terrane: Oceanic plateau and island crust accreted to the Brooks Range: *Journal of Geophysical Research*, v. 94, p. 15901–15923.
- Patton, W. W., Jr., 1973, Reconnaissance geology of the northern Yukon-Koyukuk province, Alaska: U.S. Geological Survey Professional Paper 774-A, p. A1–A17.
- Patton, W. W., Jr., and Box, S. E., 1989, Tectonic setting of the Yukon Koyukuk basin and its borderlands, western Alaska: *Journal of Geophysical Research*, v. 94, no. 11, p. 15807–15820.
- Patton, W. W., Jr., Tailleir, I. L., Brosgé, W. P., and Lanphere, M. A., 1977, Preliminary report on the ophiolites of northern and western Alaska, in Coleman, R. G., and Irwin, W. P., eds., *North American ophiolites*: Oregon Department of Geology and Mineral Industries Bulletin, v. 95, p. 51–57.
- Pavlis, T. L., 1986, The role of strain heating in the evolution of megathrusts: *Journal of Geophysical Research*, v. 91, p. 12407–12422.
- Pearce, J. A., Lippard, S. J., and Roberts, S., 1984, Characteristics and tectonic significance of supra-subduction zone ophiolites, in Kokelaar, B. P., and Howells, M. F., eds., *Marginal basin geology*: Oxford, United Kingdom, Blackwell Scientific Publications, Geological Society of London, Special Publication, v. 16, p. 77–94.
- Plafker, G., 1988, Synopsis of the Phanerozoic tectonic evolution of Alaska: *Geological Society of America Abstracts with Programs*, v. 20, p. A133.
- Raase, P., 1974, Al and Ti contents of hornblendes, indicators of temperature and pressure of regional metamorphism: *Contributions of Mineralogy and Petrology*, v. 45, p. 231–236.
- Roeder, D. H., and Mull, C. G., 1978, Tectonics of Brooks Range ophiolites, Alaska: *American Association of Petroleum Geologists Bulletin*, v. 62, p. 1696–1702.
- Rutter, E. H., 1976, The kinetics of rock deformation by pressure solution: *Philosophical Transactions of the Royal Society of London*, v. 283, p. 203–219.
- Schmid, S. M., 1992, Microfabric studies as indicators of deformation mechanisms and flow laws operative in mountain building, in Hsue, K. J., ed., *Mountain building processes*: London, Academic Press, p. 95–110.
- Searle, M. P., and Malpas, J., 1980, Structure and metamorphism of rocks beneath the Semail ophiolite of Oman and their significance in ophiolite obduction: *Transactions of the Royal Society of Edinburgh, Earth Sciences*, v. 71, p. 247–262.
- Shapiro, L., and Brannock, W. W., 1962, Rapid analysis of silicate, carbonate and phosphate: U.S. Geological Survey Bulletin, v. 1144-A, 56 p.
- Smith, A. G., 1988, Temperatures at the base of a moving ophiolite slab: The geology and tectonics of the Oman region: *International Discussion Meeting of the Geological Society of London, Edinburgh, United Kingdom: Abstracts*, p. 59.
- Snelson, S., and Tailleir, I. L., 1968, Large-scale thrusting and migrating Cretaceous foredeeps in the western Brooks Range and adjacent region of northwestern Alaska [abs.]: *American Association of Petroleum Geologists Bulletin*, v. 52, p. 567.
- Spray, J. G., 1984, Possible causes and consequences of upper mantle decoupling and ophiolite displacement, in Gass, I. G., Lippard, S. J., and Shelton, A. W., eds., *Ophiolites and oceanic lithosphere*: Oxford, United Kingdom, Blackwell Scientific Publications, Geological Society of London, Special Publication, v. 13, p. 225–268.
- Tailleir, I. L., 1970, Structure and stratigraphy of western Alaska [abs.]: *American Association of Petroleum Geologists Bulletin*, v. 54, p. 2508.
- Till, A. B., Schmidt, J. M., and Nelson, S. W., 1988, Thrust involvement of metamorphic rocks, southwest Brooks Range, Alaska: *Geology*, v. 16, p. 930–933.
- Thirwall, M. F., and Burnard, P., 1990, Pb-Sr-Nd isotope and chemical study of the origin of undersaturated and oversaturated shoshonitic magmas from the Borralan pluton, Assynt, NW Scotland: *Journal of the Geological Society of London*, v. 147, p. 259–269.
- Twiss, R. J., 1986, Variable sensitivity piezometric equations for dislocation density and subgrain diameter and their relevance to olivine and quartz, in Hobbs, B. E., and Heard, H. C., eds., *Mineral and rock deformation: Laboratory studies*: American Geophysical Union Geophysical Monograph 36, p. 247–262.
- Walsh, J. N., 1980, The simultaneous determination of the major, minor and trace constituents of silicate rocks using inductively coupled plasma spectrometry: *Spectrochimica Acta*, v. 35B, p. 107–111.
- Walsh, J. N., Buckley, F., and Barker, J., 1981, The simultaneous determination of the rare earth elements in rocks using inductively coupled plasma source spectrometry: *Chemical Geology*, v. 33, p. 141–153.
- Williams, H., and Smyth, W. R., 1973, Metamorphic aureoles beneath ophiolite suites and alpine peridotites: Tectonic implications with western Newfoundland examples: *American Journal of Science*, v. 273, p. 594–621.
- Wirth, K. R., and Bird, J. M., 1992, Chronology of ophiolite crystallization, detachment, and emplacement: evidence from the Brooks Range, Alaska: *Geology*, v. 20, p. 75–78.
- Wirth, K. R., Harding, D. J., Blythe, A. K., and Bird, J. M., 1986, Brooks Range ophiolite crystallization and emplacement ages from $^{40}\text{Ar}/^{39}\text{Ar}$ data: *Geological Society of America Abstracts with Programs*, v. 18, p. 792.
- Wirth, K. R., Harding, D. J., and Bird, J. M., 1987, Basalt geochemistry, Brooks Range, Alaska: *Geological Society of America Abstracts with Programs*, v. 19, p. 454.
- Zimmerman, J., and Frank, C. O., 1982, Possible ophiolite obduction-related metamorphic rocks at the base of the ultramafic zone, Avan Hills complex, De Long Mountains, in Coonrad, W. L., ed., *The United States Geological Survey in Alaska—Accomplishments during 1980*: U.S. Geological Survey Circular, v. 844, p. 27–28.